

DESIGNING A SILK-BASED BILAYERED MEMBRANE WITH GLASS
PARTICLES FOR DENTAL BARRIER MEMBRANE APPLICATIONS

A THESIS SUBMITTED TO
THE GRADUATE SCHOOL OF NATURAL AND APPLIED SCIENCES
OF
MIDDLE EAST TECHNICAL UNIVERSITY

BY

EZGİ YÜCEL

IN PARTIAL FULFILLMENT OF THE REQUIREMENTS
FOR
THE DEGREE OF MASTER OF SCIENCE
IN
BIOMEDICAL ENGINEERING

NOVEMBER 2024

Approval of the thesis:

DESIGNING A SILK-BASED BILAYERED MEMBRANE WITH GLASS PARTICLES FOR DENTAL BARRIER MEMBRANE APPLICATIONS

submitted by **EZGİ YÜCEL** in partial fulfillment of the requirements for the degree of **Master of Science in Biomedical Engineering, Middle East Technical University** by,

Prof. Dr. Naci Emre Altun
Dean, **Graduate School of Natural and Applied Sciences**

Prof. Dr. Vilda Purutçuoğlu
Program Coordinator, **Biomedical Engineering Program**

Assoc. Prof. Dr. Batur Ercan
Supervisor, **Metallurgical and Materials Engineering, METU**

Examining Committee Members:

Prof. Dr. Dilek S. Keskin
Engineering Sciences, METU

Assoc. Prof. Dr. Batur Ercan
Metallurgical and Materials Engineering, METU

Prof. Dr. Abdullah Öztürk
Metallurgical and Materials Engineering, METU

Assoc. Prof. Dr. Salih Özçubukçu
Chemistry, METU

Assoc. Prof. Dr. Cem Bayram
Nanotechnology and Nanomedicine,
Hacettepe University

Date: 27.11.2024

I hereby declare that all information in this document has been obtained and presented in accordance with academic rules and ethical conduct. I also declare that, as required by these rules and conduct, I have fully cited and referenced all material and results that are not original to this work.

Name Last name : Ezgi Yücel

Signature :

ABSTRACT

DESIGNING A SILK-BASED BILAYERED MEMBRANE WITH GLASS PARTICLES FOR DENTAL BARRIER MEMBRANE APPLICATIONS

Yücel, Ezgi
Master of Science, Biomedical Engineering
Supervisor : Assoc. Prof. Dr. Batur Ercan

September 2024, 62 pages

Dental barrier membranes (DBM) are widely used biomedical materials in alveolar bone defect sites for guided tissue regeneration (GTR). DBMs prevent soft tissue ingrowth into the area where regeneration of the relatively slower-growing bone tissue is desired. A DBM should have a degradation rate that matches the healing rate of the bone tissue at sites with insufficient bone, and have sufficient mechanical properties to exhibit barrier function. In this thesis, a bilayered DBM was designed and fabricated. The membrane was primarily composed of silk fibroin (SF) and silk sericin (SS), which are the two main components of silk fiber. SF possesses superior mechanical properties with a relatively lower degradation rate, while SS has poor mechanical properties and a relatively higher degradation rate. The layer on the bone regeneration side (BRS) consisted of 70 wt% SS and 30 wt% SF, to achieve a higher degradation rate. Aside from the polymer content, approximately 6.5 mol% and 1 mol% calcium- and strontium-doped glass particles (GPs) were incorporated to promote osteogenesis. Doping with osteogenic ions enhances biological functions. A high degradation rate was intended in this layer to allow the GPs to quickly interact with the juxtaposed bone tissue. The layer on the soft tissue side (STS) was composed of 60 wt% SF and 40 wt% SS to achieve a lower degradation rate and improve mechanical properties to ensure the barrier

function for a sufficient period of time. The DBM was fabricated by solvent casting and evaporation method. The second layer was cast onto the other and dried. Scanning Electron Microscopy (SEM), Orbital Emission Spectroscopy (OES), Fourier Transform Infrared Spectroscopy (FTIR) and X-Ray Diffractometer (XRD) data of GPs confirmed that amorphous particles were successfully synthesized at a particle size of approximately 350 nm. SEM images and AFM results showed that the incorporation of GPs created nanostructured roughness on the surface of the membranes. Degradation test results demonstrated that combining SS and SF in different ratios altered the degradation rates of the films compared to pure SS and SF. Tensile test results indicated that the membrane had a sufficient Young's Modulus. When MC3T3-E1 preosteoblast cells were seeded on the bilayered membranes with and without GPs, cell proliferation on the membrane containing GPs increased. The results cumulatively showed that the designed bilayered composite membrane was a potential candidate for DBM applications.

Keywords: Silk Sericin, Silk Fibroin, Glass Particles, Preosteoblast, Degradation

ÖZ

DENTAL BARIYER MEMBRAN UYGULAMALARI İÇİN CAM PARÇACIKLARI İÇEREN İPEK BAZLI ÇİFT KATMANLI MEMBRAN TASARLANMASI

Yücel, Ezgi
Yüksek Lisans, Biyomedikal Mühendisliği
Tez Yöneticisi: Doç. Dr. Batur Ercan

Eylül 2024, 62 sayfa

Dental bariyer membranlar (DBMs), alveolar kemik doku hasarının bulunduğu bölgelerde yönlendirilmiş doku rejenerasyonu (GTR) amacıyla yaygın olarak kullanılan biyomedikal malzemeledir. DBM'lar, yumuşak dokunun, göreceli olarak daha yavaş büyüyen kemik dokusunun rejenerasyonunun istendiği bölgelere taşmasını engeller. Bir DBM, yetersiz kemik dokusu bulunan bölgelerdeki kemik dokusunun iyileşme hızı ile uyuşan bir degradasyon hızına ve aynı zamanda bariyer fonksiyonunu yerine getirebilmek için yeterli mekanik özelliklere sahip olmalıdır. Bu tezde, çift katmanlı bir DBM tasarlanıp ve üretilmiştir. Membran başlıca, ipek lifinin iki ana bileşeni olan ipek fibroin (SF) ve ipek serisin (SS) bileşenlerinden oluşmaktadır. Fibroin, nispeten daha düşük bir degradasyon hızına ve üstün mekanik özelliklere sahipken, serisin daha zayıf mekanik özelliklere ve daha yüksek degradasyon hızına sahiptir. Membranın kemik rejenerasyonun gerçekleşeceği tarafındaki katman (BRS), diğer katmana kıyasla daha yüksek bir degradasyon hızı elde etmek amacıyla kütüce 70% SS ve 30% SF oranı içermektedir. Polimer içeriğinin yanı sıra, osteogenezi desteklemek amacıyla sırasıyla molce 6.5% ve 1% kalsiyum ve stronsiyum katkılı cam parçacıkları (GPs) eklenmiştir. Osteojenik iyonlar ile katkılama işlemi, biyolojik işlevlerin

geliştirilmesi için yapılmaktadır. Bu katmanda, daha yüksek degradasyon hızı, cam parçacıklarının ortam ile daha hızlı etkileşime girebilmesi için amaçlanmıştır. Yumuşak doku tarafındaki (STS) diğer katman, bariyer fonksiyonunun yeterli süre boyunca korunmasını sağlamak için daha yavaş bir degradasyon hızı ve iyileştirilmiş mekanik özellikler elde etmek amacıyla kütlece 60% SF ve 40% SS içermektedir. DBM, çözücü döküm ve buharlaştırma yöntemiyle üretilmiştir. İkinci katman diğer katman üzerine dökülerek kurutulmuştur. Cam parçacıkları için yapılan Taramalı Elektron Mikroskobu (SEM), Optik Emisyon Spektroskopisi (OES), Fourier Dönüşümlü Kızılötesi Spektroskopisi (FTIR) ve X-Işını Difraktometresi (XRD) analizleri, amorf parçacıkların yaklaşık 350 nm parçacık boyutu ile başarıyla sentezlendiğini doğrulamıştır. SEM görüntüleri ve AFM sonuçları, parçacıkların membranın yüzeyinde nanoyapılı yüzey pürüzlülüğü yarattığını göstermektedir. Degradasyon testleri, farklı oranlarda SS ve SF kombinasyonu ile üretilen filmlerin, saf SS ve SF'den farklı degradasyon hızlarına sahip olduğunu göstermiştir. Çekme testi, üretilen membranın yeterli bir Young Modülü'ne sahip olduğunu belirtmiştir. MTT sonuçlarından yola çıkılarak, MC3T3-E1 preosteoblast hücrelerinin, GP içeren ve içermeyen çift katmanlı membranlara ekildiğinde, GP içeren membranda hücre proliferasyonunun arttığı gözlemlenmiştir. Elde edilen sonuçlar, tasarlanan çift katmanlı kompozit membranın DBM uygulamaları için potansiyel bir aday olduğunu göstermektedir.

Anahtar Kelimeler: İpek Serisin, İpek Fibroin, Cam Parçacıkları, Preosteoblast, Degradasyon

To my beloved family and my true love...

ACKNOWLEDGEMENTS

First and foremost, I would like to thank to my supervisor Assoc. Prof. Dr. Batur Ercan for his guidance, advice, patience, motivation and belief in me at every stage of my MSc study. His continuous support and encouragement greatly influenced me during my studies. I am grateful to him for giving me the opportunity to work in his research group.

I would also like to thank members of Biomaterial and Nanomedicine Laboratory for their support, help and friendship along the way and fun times spent together. Their friendship and assistance made everything easier for me during stressful times. I will always feel lucky to know them, work with them and spent .

I am thankful to Yiğithan Tufan for help in FTIR and mechanical tests, Gizem Karaaslan for help in SEM and Zeynep Cemre Örsel for help in the fabrication process of glass particles. Also, I would like to thank Nilüfer Özel for her help in XRD.

Additionally, thanks to BIOMATEN and MERLAB for their help in material characterization.

Lastly, I have special thanks to my family for their endless love, support, patience, encouragement and caring throughout my whole life. They have been always there for me. I also appreciate all the love, support and encouragement I received from my love and my friends. They have always motivated me with their joy.

TABLE OF CONTENTS

ABSTRACT	v
ÖZ.....	vii
ACKNOWLEDGEMENTS	x
TABLE OF CONTENTS.....	xi
LIST OF TABLES.....	xiv
LIST OF FIGURES	xv
LIST OF ABBREVIATIONS	xviii
LIST OF SYMBOLS	xix
CHAPTERS	
1. INTRODUCTION	1
1.1. Dental Barrier Membrane.....	1
1.2. Silk Sericin	2
1.3. Silk Fibroin	4
1.4. Glass Particles as Reinforcements	7
1.5. Glycerol as Plasticizer	8
1.6. Objectives	9
2. LITERATURE REVIEW.....	11
2.1. Barrier Membranes in Dentistry	11
2.2. Silk Based Barrier Membranes for Dental Applications.....	15
2.3. Glass Particles in Guided Tissue Regeneration	17
3. EXPERIMENTAL METHODS	19
3.1. Materials	19

3.2. Extraction of Silk Sericin	19
3.3. Extraction of Silk Fibroin	20
3.4. Production of Calcium- and Strontium-Doped Glass Particles	21
3.5. Fabrication of the Bilayered DBM.....	22
3.6. Characterization of the DBM.....	23
3.6.1. Scanning Electron Microscopy (SEM).....	23
3.6.2. Atomic Force Microscopy (AFM)	23
3.6.3. X-Ray Diffraction (XRD)	24
3.6.4. Fourier Transform Infrared Spectroscopy (FTIR)	24
3.6.5. Inductively Coupled Plasma - Optical Emission Spectrometry (ICP- OES).....	24
3.6.6. Water Contact Angle Measurement	24
3.6.7. Degradation and Swelling Tests of the DBM	25
3.6.8. Mechanical Properties	25
3.7. Biological Experiments	25
3.7.1. Fibroblast Cell Culture and Cytotoxicity Evaluation	25
3.7.2 Preosteoblast Cell Culture and Evaluation of Proliferation.....	26
3.7.3. Morphologies of MC3T3-E1 Preosteoblast Cells	27
3.8. Statistical Analysis	27
4. RESULTS AND DISCUSSION.....	29
4.1. Characterization of the Fabricated GPs.....	29
4.2. Characterization of the Fabricated DBM	31
4.3. Biological Evaluation of the DBM	40
4.3.1. Cytotoxicity Evaluation of the DBM	40
4.3.2. MC3T3-E1 Preosteoblast Cell Proliferation.....	40

CONCLUSION	45
FUTURE WORK	47
REFERENCES	49

LIST OF TABLES

TABLES

Table 1.1. Abbreviations for the compositions of the films examined in this thesis.....	10
Table 2.1. Examples for non-absorbable DBMs(Solomon et al., 2022).	13
Table 2.2. Examples and classification of absorbable DBMs (Solomon et al., 2022).	13
Table 4.1. Sessile drop water contact angle results of the samples.	38

LIST OF FIGURES

FIGURES

Figure 1.1.	(a)Illustration of DBM application and (b) surface features of a DBM (Kim et al., 2023; Bee & Hamid, 2022).....	1
Figure 1.2.	Classification of DBMs (Yang et al., 2022).	2
Figure 1.3.	(a) <i>Bombyx Mori</i> silkworm cocoons and (b) the two main components of silk fiber (Ma et al., 2024; Morin et al., 2017).....	3
Figure 1.4.	(a) Structure of the SS polypeptide and (b) its amino acid composition (Cao & Zhang, 2016; Çapar & Aygün, 2015).....	3
Figure 1.5.	Amino acid sequence of the heavy chain of SF (King et al., 2023)....	4
Figure 1.6.	Schematic showing the secondary structure of SF (dos Santos et al., 2024).....	5
Figure 1.7.	Various biomaterial architectures fabricated from SF and their application areas (Johari et al., 2022).....	6
Figure 1.8.	Example of the silicate network and network modifiers for glasses used in biomedical applications (Drevet et al., 2024).	7
Figure 1.9.	Various properties of GPs doped with additional elements (Al-Harbi et al., 2021).	7
Figure 1.10.	(a) Structure and (b) atomic model of the glycerol molecule (Özeren et al., 2020; Tan et al., 2013).	9
Figure 2.1.	Schematic illustrating the stages of periodontitis (PDL: Periodontal ligament) (Bee & Hamid, 2022).....	11
Figure 2.2.	Illustration of DBM application (a) without bone graft, and (b) with bone graft (Alqahtani, 2023; Ko et al., 2016).	12

Figure 2.3.	Example for a multifunctional DBM with varying chemical compositions in its layers (Assadi et al., 2024).....	15
Figure 2.4.	Flexible SS film achieved by the addition of glycerol (Yun et al., 2016).....	17
Figure 2.5.	Effects of doping GPs with strontium ion on its biological properties (A. V. Silva et al., 2023).....	18
Figure 3.1.	Extraction of SS from the cocoons via the autoclave method.	20
Figure 3.2.	Extraction steps of SF from cocoons.	21
Figure 3.3.	Fabrication of GPs via the Stöber method.	22
Figure 3.4.	Fabrication steps of the bilayered DBM.	23
Figure 4.1.	(a) SEM images and (b) ICP-OES results showing the composition of the GPs.....	29
Figure 4.2.	XRD spectrum of the fabricated GPs.	30
Figure 4.3.	FTIR spectrum of the fabricated GPs.....	31
Figure 4.4.	Flexibility of the fabricated DBM.	31
Figure 4.5.	XRD spectra of pure SF, STS and BRS layers of the DBM, and pure SS.....	32
Figure 4.6.	FTIR spectra of pure SF, STS and BRS layers of the DBM, and pure SS.....	33
Figure 4.7.	SEM images of the cross-section of the DBM (left), and top surfaces of the BRS and STS layers of the DBM.	34
Figure 4.8.	(a) AFM images of BRS (left) and STS (right), and (b) graph indicating the RMS values of BRS and STS. *p< 0.05.....	35

Figure 4.9. % Swelling values of SF, STS, BRS, 70SS/30SF and DBM samples in 1x PBS upon 4 h of immersion time. Values are mean \pm SD (n=3), *p< 0.05.....	36
Figure 4.10. % Weight loss for pure SF, STS, BRS, 70SS/30SF and DBM samples in 1x PBS up to 2 weeks.....	37
Figure 4.11. (a) Stress-strain graphs and (b) Young's modulus values of the STS, BRS and DBM samples calculated from the elastic region of the stress-strain graph. Values are mean \pm SD (n=3), *p< 0.05.....	39
Figure 4.12. Viability of L929 fibroblasts up to 5 days in vitro. Cells were incubated with the extract of the DBM. Values are mean \pm SD, n=3. *p< 0.05, ns: non-significant.....	40
Figure 4.13. Proliferation of MCT3-E1 preosteoblasts up to 7 days in vitro. Cells were seeded directly on the DBM. Values are mean \pm SD, n=3. *p< 0.05, ns: non-significant.	41
Figure 4.14. Attached cells on the membrane (a) without and (b) with GPs, respectively	42

LIST OF ABBREVIATIONS

ABBREVIATIONS

DBM	: Dental Barrier Membrane
SS	: Silk Sericin
SF	: Silk Fibroin
GP	: Glass Particles
GTR	: Guided Tissue Regeneration
GBR	: Guided Bone Regeneration
Ca	: Calcium
Sr	: Strontium
CaN	: Calcium Nitrate
SrN	: Strontium Nitrate
SEM	: Scanning electron microscopy
XRD	: X-Ray Diffraction
FTIR	: Fourier Transform Infrared Spectroscopy
AFM	: Atomic Force Microscopy
OES	: Optical Emission Spectroscopy
PBS	: Phosphate Buffer Saline
RMS	: Root Mean Square
SD	: Standard Deviation

LIST OF SYMBOLS

SYMBOLS

nm	: nanometer
mL	: milliliter
L	: liter
rpm	: revolutions per minute
g	: gram
min	: minute
h	: hour
θ	: Theta

CHAPTER 1

INTRODUCTION

1.1. Dental Barrier Membrane

Dental barrier membranes (DBMs) are frequently used in dental applications for guided tissue regeneration in areas of alveolar bone defects caused by a periodontal disease (Periodontitis). Periodontitis is a treatable disease; however, its complications can cause permanent damage to the alveolar bone and periodontal tissue, potentially leading to tooth loss (Kim et al., 2023). A DBM is placed between the soft tissue and the bone defect area to prevent the faster-growing soft tissue ingrowing into the defect site. In addition to providing space for tissue reconstruction, the ability to support tissue regeneration is also a preferred feature for a barrier membrane, as shown in Figure 1.1.

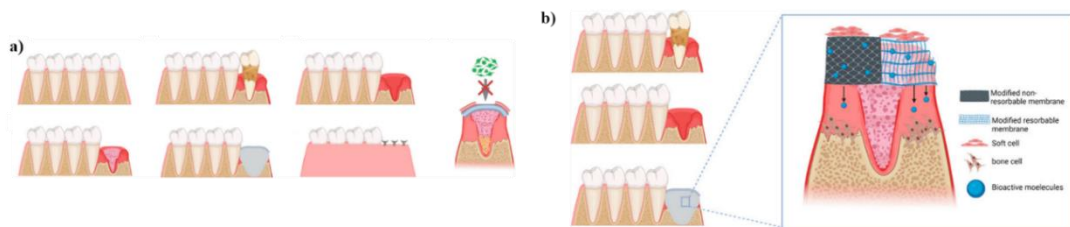


Figure 1.1. (a) Illustration of DBM application and (b) surface features of a DBM (Kim et al., 2023; Bee & Hamid, 2022).

Due to the need for barrier membranes to prevent soft tissue overgrowth while promoting bone tissue regeneration, there has been an increasing demand for multilayered asymmetric membranes with different layer compositions, depending on the tissue they will interact with (Bee & Hamid, 2022).

Dental Barrier Membrane can be classified in two main groups; non resorbable (non absorbable) and resorbable (absorbable) membranes, as indicated in Figure 10

(Yang et al., 2022). Additionally, resorbable membranes can be divided into two subclasses as natural and synthetic membranes (Zheng et al., 2019).

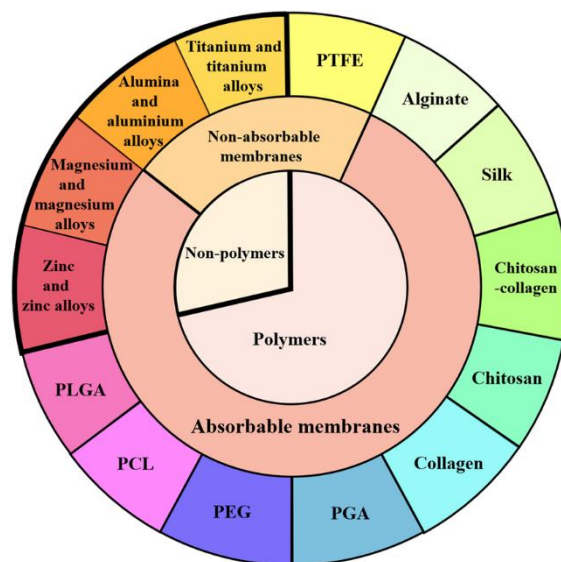


Figure 1.2. Classification of DBMs (Yang et al., 2022).

1.2. Silk Sericin

Silk sericin (SS) is one of the two main components of silk cocoons fabricated from *Bombyx Mori* silkworm which plays a crucial role in preserving the structural integrity of cocoons, as shown in Figure 1.1 (Babu & Suamte, 2024). 20-30% of the silk fiber is composed of sericin (Rocha et al., 2017). For many years, SS has been discarded as silk industry waste in contrast with fibroin due to the superior mechanical properties of fibroin (Liu et al., 2022). However, in last years, SS has gained significant interest for biomedical applications due to its outstanding biocompatibility, biodegradability, and ability to promote fibroblast cell attachment, growth and differentiation (He et al., 2017; Hu et al., 2023; Liu et al., 2022). Also, SS is an extremely hydrophilic polymer attributed to its amino acid content (He et al., 2017). Nevertheless, SS alone is not very suitable for biomedical applications because of its brittleness and poor mechanical properties. To overcome these disadvantages, one effective method is blending sericin with another polymer or a plasticizer (He et al., 2017; Yun et al., 2016).

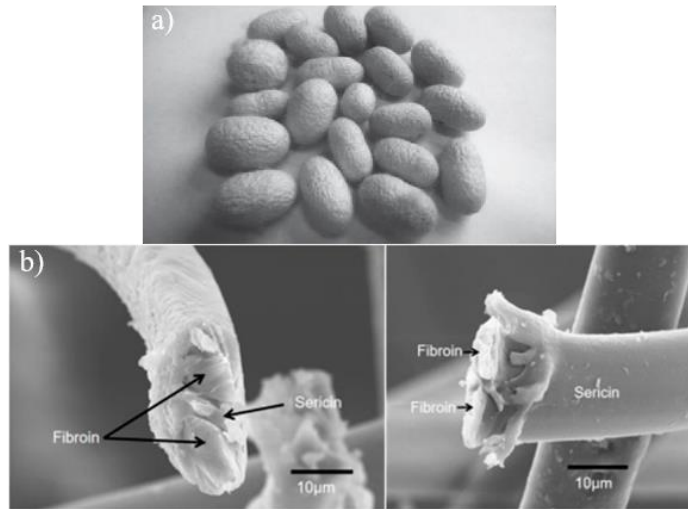


Figure 1.3. (a) *Bombyx Mori* silkworm cocoons and (b) the two main components of silk fiber (Ma et al., 2024; Morin et al., 2017).

SS is a globular water-soluble protein and has a molecular weight ranging from 20 kDa to 400 kDa (Rocha et al., 2017). It shows a layered structure in cocoons and the outermost layer is the one that dissolves most easily in high temperatures, such as hot water due to its amino acid content (Cao & Zhang, 2016). The amino acid composition of SS is largely composed of hydrophilic and polar amino acids such as serine, aspartic acid and contains high concentration of hydroxyl, carboxyl and amino groups which gives its water solubility, as seen in Figure 1.2 (Cao & Zhang, 2016).

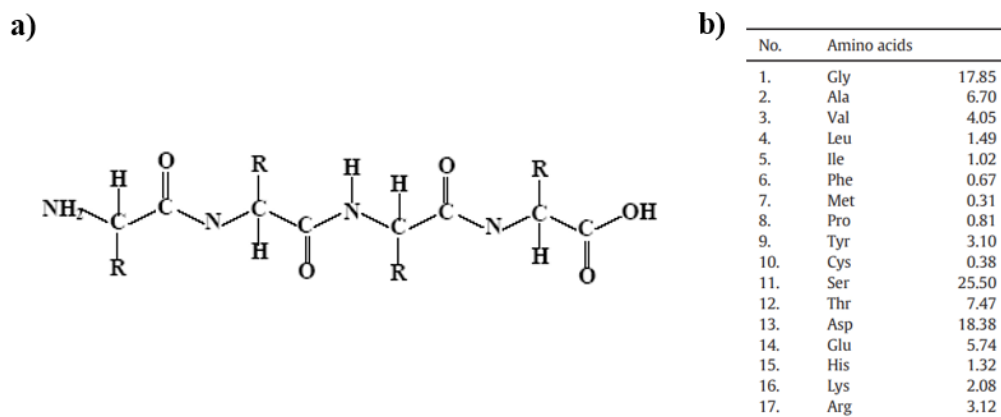


Figure 1.4. (a) Structure of the SS polypeptide and (b) its amino acid composition (Cao & Zhang, 2016; Çapar & Aygün, 2015).

There are variable extraction methods of SS from cocoons such as extraction with boiling water, alkaline extraction, extraction with autoclave (High temperature and high pressure method) and aqueous extraction in mild conditions. According to extraction process, secondary structure content of SS can vary (Chirila et al., 2016). Autoclave method generally yields in higher β -sheet amount in the structure of SS compared to other common methods. Also, this method helps to extract SS more efficiently and rapidly with higher purity when compared to other methods which often require longer processing times or various chemicals. Moreover, it is an environmentally friendly process (Gaviria et al., 2023; A. S. Silva et al., 2022).

1.3. Silk Fibroin

Bombyx mori silk mainly consists of sericin and fibroin. Silk fibroin (SF) has emerged as a promising material for tissue engineering applications due to its desirable properties including elasticity, mechanical strength, tunable degradation rates and biocompatibility (Liu et al., 2022). SF is composed of light (L) and heavy (H) chain polypeptides which are connected by a disulfide bond, making a H-L complex. Additionally, P25 glycoprotein is linked to H-L complex non-covalently and plays crucial role in preserving the integrity of the complex (Kundu et al., 2013). Heavy chain is mainly composed of glycine, alanine and serine (Koh et al., 2015), as shown in Figure 1.5.

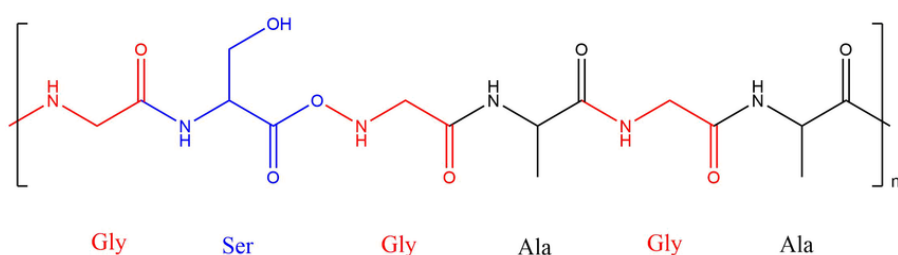


Figure 1.5. Amino acid sequence of the heavy chain of SF (King et al., 2023).

H chains contain hydrophobic domains which gives SF its hydrophobic nature, composed of Gly-X repeats where X represents Ala, Ser, Thr or Val, assembling into antiparallel β -sheet nano-crystals which contribute to the mechanical strength

of fibroin. Hydrophobic domains are linked by hydrophilic links containing bulky and polar side chains, as represented in Figure 1.5 and forming semi-crystalline structure in SF. These links result in amorphous regions with random coil chain conformation and enhance the elasticity of fibroin. Tuning the number, size, distribution, orientation and spatial arrangement of crystalline and non-crystalline domains alters the mechanical properties leading to vigorous mechanical properties and controllable degradation rates in fabricated materials (W. Huang et al., 2018; Kundu et al., 2013).

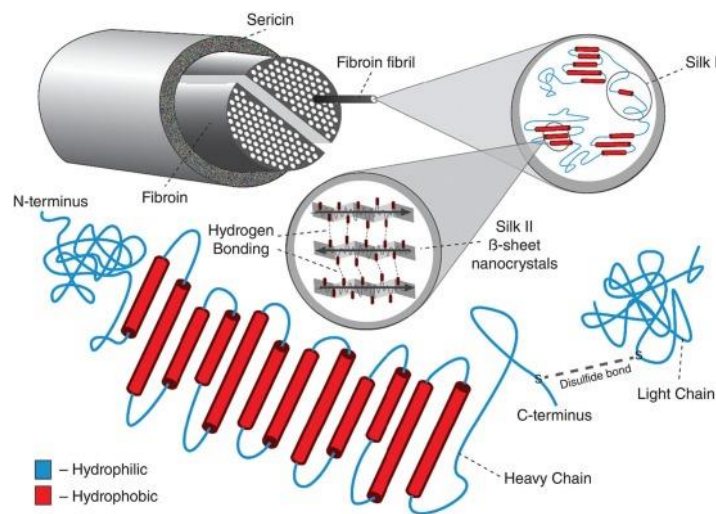


Figure 1.6. Schematic showing the secondary structure of SF (dos Santos et al., 2024).

Silk I and silk II structures represented in the figure 1.6 are the structures found in both SF and SS in the solid states. Silk I is the soluble structure of the polymer chains in the middle glands of the silkworms. If SF dries without any external forces, it mainly possesses silk I structure. On the other hand, silk II is the crystalline structure of SF, formed after spinning process. It is the insoluble form of SF chains. While silk I mainly composed of random coils and α -helices, silk II is predominantly composed of β -sheet secondary structures. The amounts of silk I and silk II structures can be adjusted in the fabricated materials by altering crystallization. (Asakura & Williamson, 2023; Huang et al., 2023).

According to extraction method of SF from silk cocoons, properties of final biomaterial can be varied. Alkaline degumming process for the extraction of fibroin is a rapid, efficient and environmentally friendly method. Furthermore, it is a mild method which minimizes the risk of damaging the molecular structure and integrity of fibroin, ensuring that the extracted SF retains its properties (Carissimi et al., 2019).

Fabrication of SF primarily includes degumming process, dissolution, dialysis and centrifugation. After processing, obtained SF can be used to form numerous material types for biomedical applications such as tissue engineering and drug delivery systems, as shown in Figure 1.6 (Johari et al., 2022; Rockwood et al., 2011).

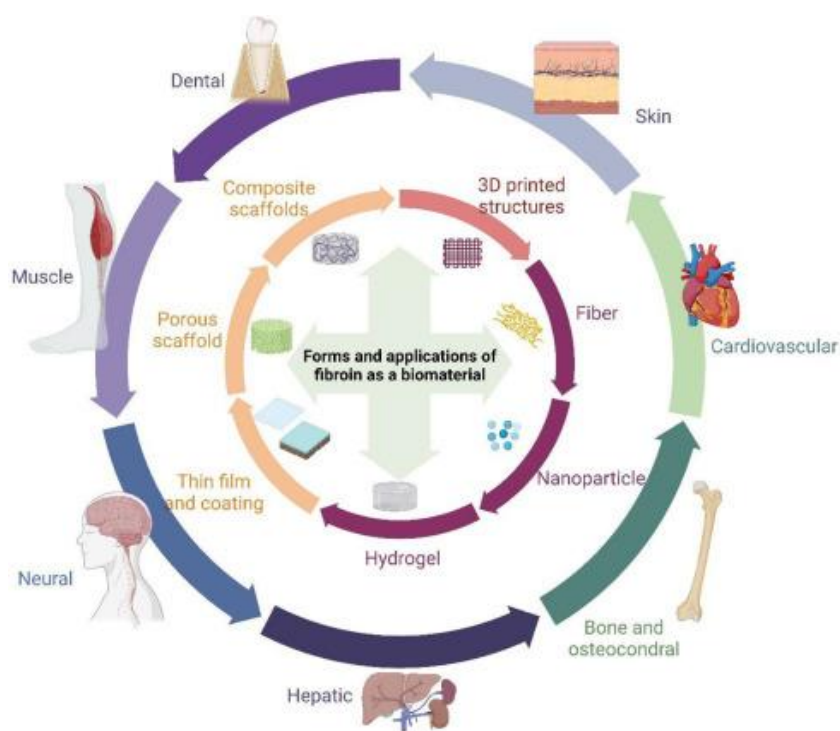


Figure 1.7. Various biomaterial architectures fabricated from SF and their application areas (Johari et al., 2022).

1.4. Glass Particles as Reinforcements

Glass particles (GPs) used in biomedical applications are biocompatible ceramic materials that are composed of a silicate network incorporated with elements such as calcium or sodium as network modifiers, depending on the desired properties, as shown in Figure 1.7.

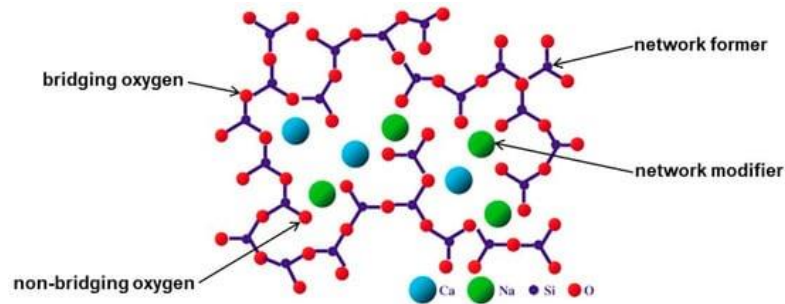


Figure 1.8. Example of the silicate network and network modifiers for glasses used in biomedical applications (Drevet et al., 2024).

Besides, additional elements can also be incorporated into the glass structure such as strontium, zinc, magnesium or silver, thereby imparting various properties to GPs and elevating their biological properties (Boccaccini et al., 2010; Taye, 2022). These elements can enhance the ability to support bone formation or impart antibacterial properties, as illustrated in Figure 1.8. (Boccaccini et al., 2010).

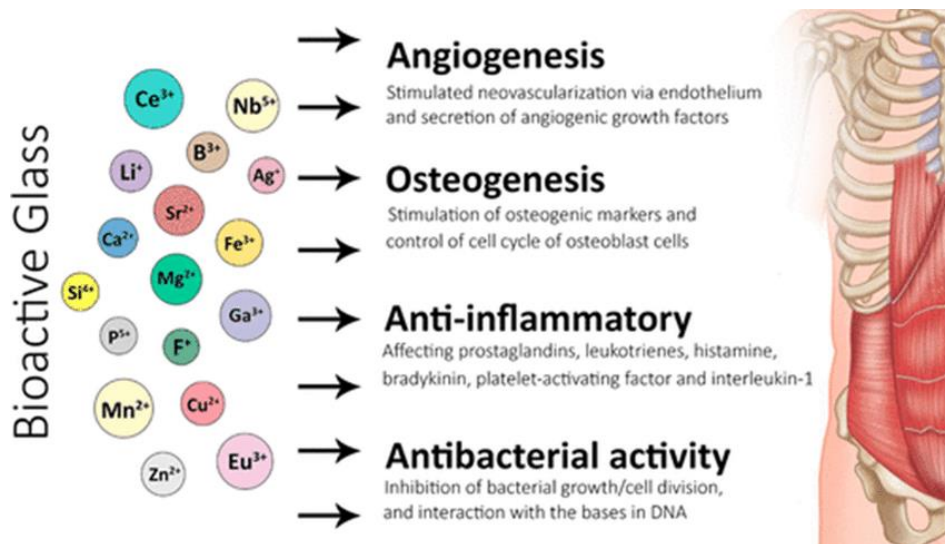


Figure 1.9. Various properties of GPs doped with additional elements (Al-Harbi et al., 2021).

Most commonly used methods for the fabrication of GPs are sol-gel and melt quenching methods. Owing to its fine control over synthesis parameters and low-temperature processing, the sol-gel method is favored over melt quenching for fabricating GPs with well-defined structural properties (Pawar & Shinde, 2024).

GPs promote osteogenesis as a result of their chemical compositions, releasing ions during degradation (Wu et al., 2022). Also, studies showed that altering surface area/volume ratio of GPs affects their bioactivity, hydrophilicity and mechanical properties (Tamjid et al., 2011). Yet, stiffness and brittle nature of these materials restricts their usage in load bearing applications such as bone tissue engineering. Thus, blending GPs with polymers makes it possible to overcome the disadvantages of GPs and focus on their benefits (Wu et al., 2022).

GPs are widely being used as reinforcements in polymer matrices, especially in bone tissue engineering applications, wound healing and drug delivery applications (Barreto et al., 2023; Tamjid et al., 2011; Vallittu et al., 2015; Wu et al., 2022; Zeimaran et al., 2015). Usage of GPs as reinforcements in composites, can also enhance mechanical properties of polymers to suitable levels for bone regeneration studies, besides improving biological properties of the polymers (Niknafs et al., 2024; Xu et al., 2023; Zeimaran et al., 2015).

1.5. Glycerol as Plasticizer

To elevate mechanical properties such as flexibility and processability polymers, plasticizers can be blended as additives. Glycerol is one of the most prevalently used non-toxic plasticizer for enhancing elongation of polymers considering its effectiveness (Yun et al., 2016). Glycerol addition can provoke β -sheet formation in the secondary structure of silk based biopolymers and nevertheless results in flexible material. Hydroxyl groups of glycerol molecule which can be seen in Figure 1.9, are thought to inspire this effect (Brown et al., 2016). There are few theories about the mechanism of the plasticizing effect of Glycerol. Because glycerol is a small molecule, it is able to enter between the polymer chains. As explained in Glass Theory, glycerol disrupts interactions between polymer chains

such as hydrogen bonds. As a result, free volume and freedom of motion of polymer chains increases, leading to enhanced flexibility and lower glass transition temperature (Żołek-Tryznowska & Cichy, 2018).

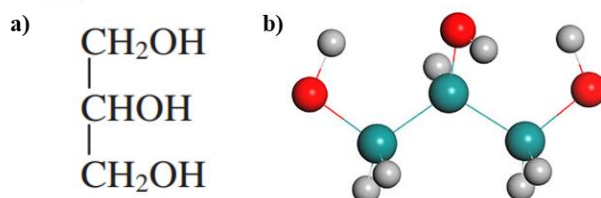


Figure 1.10. (a) Structure and (b) atomic model of the glycerol molecule (Özeren et al., 2020; Tan et al., 2013).

1.6. Objectives

The aim of this work is to design a bilayered membrane with suitable degradation and mechanical properties for dental barrier membrane applications by combining silk sericin, silk fibroin and glass particles. Combination of silk sericin and silk fibroin in order to fabricate a bilayered membrane and incorporation of calcium- and strontium-doped glass particles to be used in dental barrier membrane applications were not investigated previously in literature. Sericin and fibroin solutions were fabricated separately and recombined in order to reduce the risk of allergic reactions for patients causing from the antigen-like conformations in the native form of these polymers in cocoons (Long et al., 2021). Glass particles are doped with calcium and strontium for the enhancement of the osteogenic properties. The polymer ratios of the layers of the membrane differ depending on the intended function of each layer. The layer on the bone regeneration side is composed of higher sericin amount to increase the degradation rate for rapid ion release from glass particles for the improvement of the preosteoblast proliferation. The other layer on the soft tissue side is consist of a higher fibroin content in order to ensure the maintenance of the barrier function of the membrane for a sufficient period of time.

The research objective of this theses are:

- To design and fabricate a degradable composite bilayered membrane to be used as dental barrier membrane,
- To characterize the fabricated membrane,
- To investigate the cytotoxicity of the membrane and explore the effects of the membrane on the proliferation of preosteoblast cells.

Table 1.1. Abbreviations for the compositions of the films examined in this thesis.

Abbreviation	Composition
Silk Sericin (SS)	Pure sericin
Silk Fibroin (SF)	Pure fibroin
70SS/30SF	70 wt% SS + 30 wt% SF (+ 30 wt% glycerol with respect to total polymer content)
70SS/30SF/GP (Bone regeneration side "BRS")	70 wt% SS + 30 wt% SF (+ 10 wt% GP and 30 wt% glycerol with respect to total polymer content)
40SS/60SF (Soft tissue side "STS")	40 wt% SS + 60 wt% SF (+ 30 wt% glycerol with respect to total polymer content)
Dental Barrier Membrane (DBM)	Bilayered membrane with BRS and STS

CHAPTER 2

LITERATURE REVIEW

2.1. Barrier Membranes in Dentistry

Periodontitis is a inflammatory disease that cause damage to the tissues surrounding and supporting the teeth, leading to loss of alveolar bone and connective tissue, illustrated in Figure 2.1. Also, genetic factors, environmental factors and certain health conditions such as diabetes, pulmonary disease or cardiovascular disease can give rise to this disorder (Pihlstrom et al., 2005). If left untreated, it leads tooth loss. A survey of Centers for Disease Control and Prevention, nearly half of the U.S. adult population is suffering from this disease (Bee & Hamid, 2022). It is considered one of the most common infection among humans (Nasajpour et al., 2018).

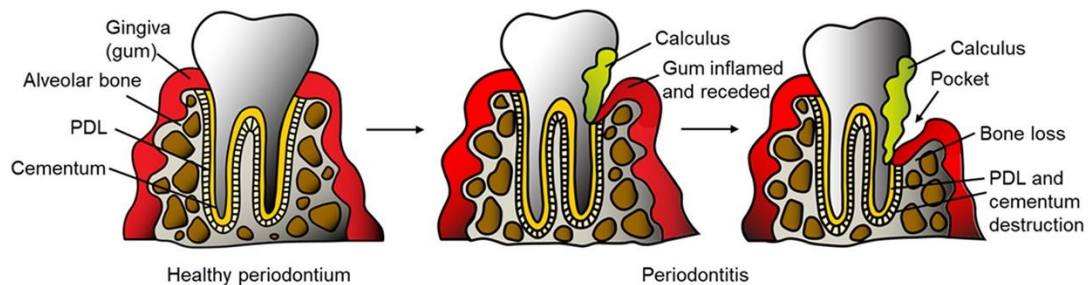


Figure 2.1. Schematic illustrating the stages of periodontitis (PDL: Periodontal ligament) (Bee & Hamid, 2022).

Dental regenerative treatments including guided tissue regeneration (GTR) and guided bone regeneration (GBR) are highly used for restoring the affected tissue. In these treatments, DBMs are used in bone reconstruction areas, as shown in Figure 2.2 (Bee & Hamid, 2022). DBMs can be used to restore damaged tissue with or without bone grafts (Dogan et al., 2003).

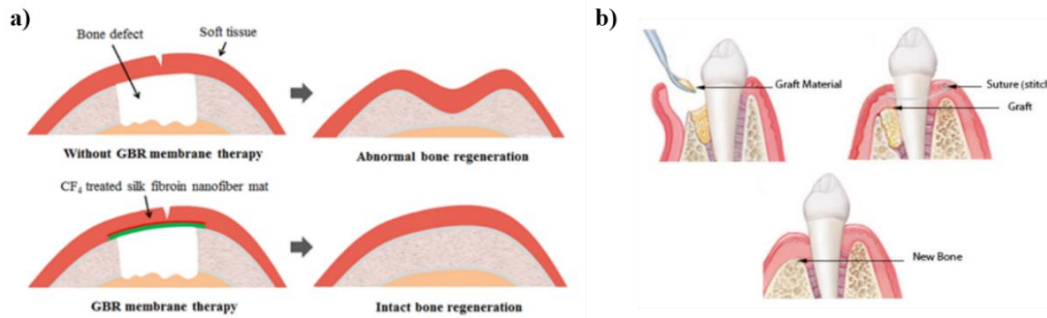


Figure 2.2. Illustration of DBM application (a) without bone graft, and (b) with bone graft (Alqahtani, 2023; Ko et al., 2016).

DBMs are placed between soft epithelium tissue and bone defect area to prevent soft tissue invasion into the bone regeneration area and maintain that space for bone tissue growth. DBMs should possess sufficient mechanical properties, in order to resist the pressure of the growing soft tissue and maintain its barrier function for the required duration (Sasaki et al., 2021). Although it varies depending on the specific application, the membrane is expected to persist its barrier function for 4-6 weeks for periodontal regeneration and 16-24 weeks in bone augmentation (Caballé-Serrano et al., 2017; Hoornaert et al., 2016). Along with the mechanical properties of the membrane, its biological properties are also important, especially in third generation barrier membranes.

Commercialized DBMs can be classified as absorbable and non-absorbable membranes. Non-absorbable membranes such as titanium mesh, high density polytetrafluoroethylene (d-PTFE) or expanded polytetrafluoroethylene (e-PTFE) are generally included in first generation membranes, shown in Table 2.1.

Table 2.1. Examples for non-absorbable DBMs(Solomon et al., 2022).

Composition		Commercial Variants	Observations
Titanium		Osteo-Mesh TM-300®	Very good mechanical properties Bio-inert High risk of oral exposure Requires setting pins Requires second surgical time
		Frios BoneShields	
Silicone			Low cost Bio-inert Very low micro-porosity Requires second surgical time
Polytetrafluoroethylene (PTFE)	Expanded (e-PTFE)	Gore-Tex®	Good mechanical properties Good micro-porosity Bio-inert High risk of oral exposure, with bacterial loading
	High density (d-PTFE)	High density Gore-Tex® Cytoplast TXT-200® Cytoplast Regentex GBR-200®	Good mechanical properties Good micro-porosity Smooth surface (low risk of bacterial loading) Can be left partially exposed in the oral cavity High risk of oral exposure
	e-PTFE with titanium	Gore-Tex® Reinforced	Very good mechanical properties Bio-inert
	d-PTFE with titanium	Cytoplast Regentex Ti-250®	High risk of oral exposure

On the other hand, absorbable membranes which eliminates second surgical operation for the removal of the membrane, are considered second generation membranes. Synthetic and natural membranes are the two subgroups of the second generation membranes, shown in Table 2.2 (Alqahtani, 2023)

Table 2.2. Examples and classification of absorbable DBMs (Solomon et al., 2022).

Type	Commercial Variants		Absorption Time	Observations	
Natural	Proteins	BioGide®	24 weeks	From porcine dermis Composition: type I and III collagen	
		Periogen®	4-8 weeks		
		RCM	26-38 weeks		
		BioMend®	6-8 weeks	From bovine tendon Composition: 100% type I collagen	
		BioMend-Extend®	18 weeks		
		OSSIX®	6 months		
	Fibrin	Paroguide®	4-8 weeks	From calfskin Composition: 96% type I collagen, 4% chondroitin-4-sulfate	
		Alloderm®	8-10 weeks	From human cadaver Composition: type I collagen	
		Autologous	7-11 days	Elastin and bovine fibrin with a polyglactin mesh	
		Etik-Patch®	4-6 weeks		
Polysaccharides	Chitosan	16-20 weeks			
	Cellulose	Nanoskin®			
	Alginate				
	Agarose				
Synthetic	PGA/TMC	Resolut Adapt X®	16-24 weeks		
		Resolut Adapt LT®			
	PLA	Polylactic acid	Guidor® Epi-guide®		10-12 weeks
		PLA/PGA/TMC	Resolut Adapt®		8-10 weeks

PGA: polyglactic acid; PLA: polylactic acid; TMC: trimethyl chitosan

Recently preferred DBMs are usually third generation barrier membranes which have improved biological properties through the inclusion of additional materials including growth factors, antimicrobial factors and inorganic compounds. Membranes supporting tissue regeneration or showing antibacterial properties can be manufactured (Solomon et al., 2022). For instance, Mota et al. fabricated chitosan/bioactive glass composite membrane and showed that membrane with bioactive glass nanoparticles enhanced proliferation of Human Periodontal Ligament cells (hPDL) compared to the pure chitosan membrane. There was a significant difference between DNA concentrations correlated with cell proliferations of hPDL cells interacted with the pure and composite membranes (Mota et al., 2012). In another study, Nasajpour et al. produced a multifunctional membrane composed of poly(caprolactone) (PCL) and zinc oxide (ZnO) nanoparticles by electrospinning method. Antibacterial activity against *P. gingivalis* enhanced by the incorporation of ZnO particles (Nasajpour et al., 2018). Also, the impacts of combining polymers with elements such as iron, magnesium or strontium are studied. As an example, Luz et al. studied on cellulose membranes releasing strontium for guided bone regeneration (Luz et al., 2020). Strontium contributes in bone metabolism through the induction of osteogenesis, stimulation of differentiation and proliferation markers and reduction of apoptosis (Solomon et al., 2022).

Lately, in addition to mechanical properties, a remarkable attention has been given to the biological properties of barrier membranes such as osteogenic potential for effective treatments. Considering that each side of the DBM interacts with different types of tissues and biological environments, asymmetric multilayer barrier membranes that meet the required properties for both environments are highly preferred. Surface properties, morphologies or compositions may vary between the layers, depending on the intended function of different layers within the membrane (Bee & Hamid, 2022), as represented in Figure 2.3. As an example, Zhou & Li et al., designed and fabricated an asymmetric bilayered DBM possessing a bone defect side layer loaded with demineralized dentin matrix particles (DDM) and

having larger pore sizes by electrospinning. The other layer presents a smoother surface with smaller pore sizes for inhibiting the penetration of the soft tissue. Results showed that designed membrane restricts cell migration. Additionally, it was confirmed that membrane is cytocompatible and its bone defect side containing demineralized dentin matrix supported proliferation of preosteoblasts, especially at specific concentrations of dentin matrix (Zhou & Li, 2024). In another study, Gürbüz et al. manufactured a multifunctional DBM consist of three layers by electrospinning, solventcasting and particulate leaching. The innermost layer that will interface with bone regeneration area is composed of PCL/collagen-bone morphogenic protein 7 (BMP-7) and enhances MC3T3-E1 preosteoblast cell differentiation. Microporous middle layer contains PCL/nano-hydroxyapatite for supporting barrier function while simultaneously allowing bone ingrowth. Lastly, the outermost layer is consist of PCL/collagen and intended to exhibit barrier function for epithelium (Gürbüz et al., 2016).

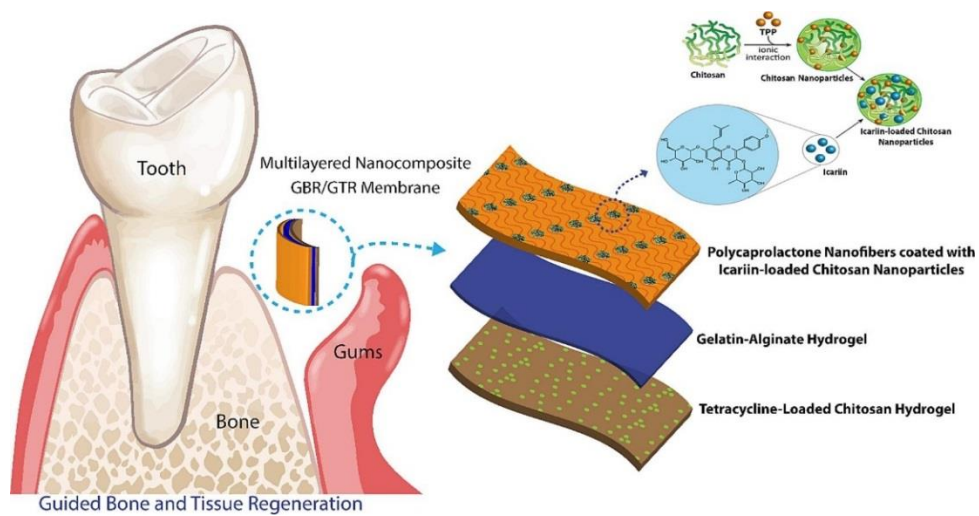


Figure 2.3. Example for a multifunctional DBM with varying chemical compositions in its layers (Assadi et al., 2024).

2.2. Silk Based Barrier Membranes for Dental Applications

Natural polymers are highly preferred in dental barrier membrane applications due to their degradability since it is a desirable feature to eliminate second surgical operation for patients.

Although the mechanical properties of natural polymers are generally weak, SF is a favored candidate for barrier membrane applications owing to its superior mechanical properties, in addition to its biocompatibility. Moreover, SF eliminates disease transmission chance when compared to human- or animal-driven biomaterials (Smeets et al., 2017). Lu et al. produced a SF nanofibrous membrane incorporated with hydroxyapatite nanoparticles possessing appropriate mechanical stability and suitable degradability. Furthermore, it has been demonstrated that the membrane enhanced bone tissue regeneration (Lu et al., 2015). In another study, Luo et al. produced an ecofriendly silk fibroin/collagen blend membrane with sufficient mechanical properties and degradation rate. In addition, produced membrane supported MC3T3-E1 preosteoblast cell adhesion and proliferation. It was also tested in vivo for 9 weeks and showed appropriate degradation rate (Luo et al., 2021).

SS, the other main component of cocoons, is a by-product in textile industry generated during the production of silk fabric from SF. SS is separated from SF through degumming process, whereby the SS is removed and generally discarded as a waste. This leads to environmental pollution due to significant oxygen consumption required for its microbial degradation. It is calculated that around 50.000 tons of SS could be recovered from the wastewater (Aramwit et al., 2012). For this reason, expanding the application areas of SS could benefit both environment and economy (Orlandi et al., 2020). SS can be used in food engineering, cosmetics, pharmaceutical or biomedical applications due to its biocompatibility, hydrophilicity and biodegradability (Orlandi et al., 2020; A. S. Silva et al., 2022). Due to the detrimental effect of by-product SS on water resources and its potential applications in various other fields, there has been an increasing demand in finding alternative application areas (A. S. Silva et al., 2022). Despite its advantageous properties, applications of SS are limited due to its brittleness. In order to overcome this limitation, SS can be blended with a plasticizer, as shown in Figure 2.9. Glycerol is one of the most commonly used

plasticizer to enhance the flexibility of SS owing to its non-toxic properties in biological environments (Yun et al., 2016; Zhang et al., 2011).



Figure 2.4. Flexible SS film achieved by the addition of glycerol (Yun et al., 2016).

Also, low mechanical strength and rapid degradation of SS restricts its usage in areas where materials with higher mechanical strength and integrity are desired. This can also be overcome by blending it with other polymers or incorporating reinforcements (He et al., 2017; Ming et al., 2022). Ming et al. fabricated an absorbable membrane composed of SS, PVA and hydroxyapatite (HAp) nanoparticles that promotes osteogenic differentiation of periodontal ligament stem cells to be used in guided tissue regeneration applications (Ming et al., 2022).

Additionally, when SS is blended with more hydrophobic polymers, it enhances the water retention ability of the resultant material owing to the hydrophilic nature of SS (K. Wang et al., 2023).

2.3. Glass Particles in Guided Tissue Regeneration

Composite membranes consisting of polymers and reinforcements such as hydroxyapatite (HAp) or glass nanoparticles (GPs) are frequently preferred because of the improvement of biological properties by the additives. Studies have shown that incorporating GPs to polymers promotes the formation of new tissue, especially when doped with ions that enhance the osteogenesis of cells such as calcium, strontium or magnesium (Mouriño et al., 2019; Taye, 2022; Xu et al., 2023), as illustrated in Figure 2.10. Easy doping with additional ions attracted interest for GPs to be used in tissue regeneration applications, in addition to

biocompatibility, bioactivity and degradability of the GPs (Vichery & Nedelec, 2016; Zhu et al., 2012).

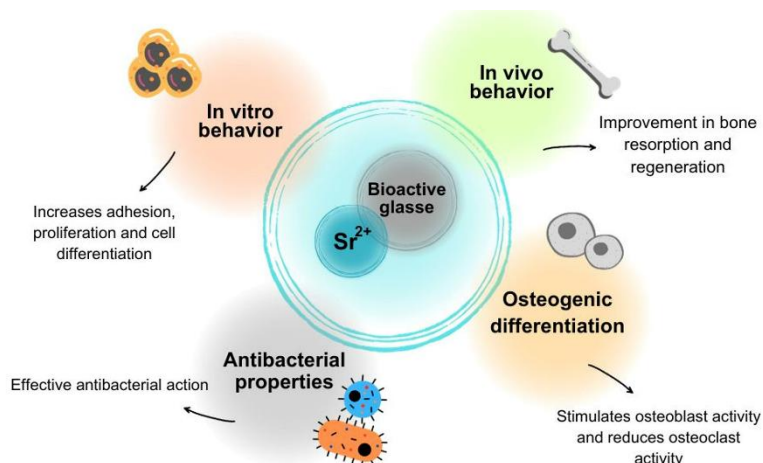


Figure 2.5. Effects of doping GPs with strontium ion on its biological properties (A. V. Silva et al., 2023).

Niknafs et al. fabricated a silk fibroin/bacterial nanocellulose scaffold incorporated with strontium-doped bioactive glass nanoparticles to enhance bone tissue regeneration. The scaffold showed improved mechanical properties. Besides, incorporation of bioactive glass particles elevated cell viability. Also in another study, Matic et al. fabricated strontium- and magnesium-doped bioactive glass particles and examined their biological properties. Results indicated that the cell proliferation was significantly improved (Matic et al., 2024).

CHAPTER 3

EXPERIMENTAL METHODS

3.1. Materials

Bombyx mori silk worm cocoons were purchased from Kozabirlik. Glycerol solution, ethanol, sodium carbonate (Na_2CO_3), lithium bromide (LiBr), calcium nitrate tetrahydrate ($\text{Ca}(\text{NO}_3)_2 \cdot 4\text{H}_2\text{O}$), tetraethyl orthosilicate (TEOS), strontium nitrate ($\text{Sr}(\text{NO}_3)_2$), hydrochloric acid (HCl), isopropanol and hexamethyldisilazane (HMDS) were obtained from Sigma Aldrich. , Dulbecco's Modified Eagle Medium (DMEM), fetal bovine serum (FBS), penicillin-streptomycin, L-glutamin and tyripsin-EDTA used in culture experiments were obtained from Biological Industries. Minimum essential medium (MEM) was purchased from Gibco. 3-(4,5-dimethyl-2-thiazolyl)-2,5-diphenyltetrazolium bromide (MTT) was purchased from Merck.

3.2. Extraction of Silk Sericin

For the extraction of SS from cocoons, autoclave method (extraction under high temperature and pressure) was used. *Bombyx Mori* cocoons were cut and the obtained pieces were put in a bottle with DI water. For each gram of cocoons, 10 mL DI water was used. Then, the bottle was put into autoclave at 121 °C for 20 minutes. As a result, SS solution was acquired. Subsequently, SS solution was put in centrifuge at 7830 rpm for about 10 minutes for the removal of unwanted remains from silkworms and cocoons. At the end, from 1 gram of cocoon, nearly 6 mL SS solution consists of approximately 0.16 g SS solution was obtained. It is important to prepare SS solution freshly just before the experiment due to the rapid gelation of SS solution as the temperature decreases.

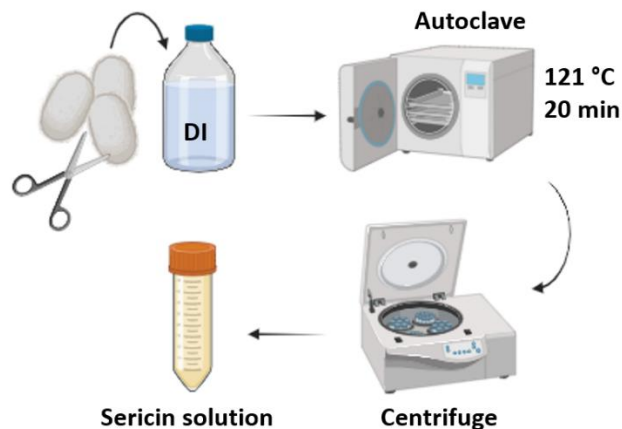


Figure 3.1. Extraction of SS from the cocoons via the autoclave method.

3.3. Extraction of Silk Fibroin

To extract SF from cocoons, firstly, sericin around the cocoons were removed by boiling 10 grams of cut cocoons in 4 liters of 0.02 M Na_2CO_3 solution at 100 °C for 30 min. The solution was stirred every 5 min to distribute the cocoons homogeneously in Na_2CO_3 solution and wet them equally for an effective extraction. The obtained fibroin was dried for 1 day inside a fume hood. Afterwards, the dried SF was dissolved in 11 M LiBr solution at 60 °C for 4 h. Then, the acquired solution was dialyzed in distilled water for 4 days to eliminate Li^+ and Br^- from the solution. Finally, dialyzed solution was centrifuged at 7830 rpm at 4 °C for 20 min to remove impurities. Generated SF solution could be stored at 4 °C for a month.

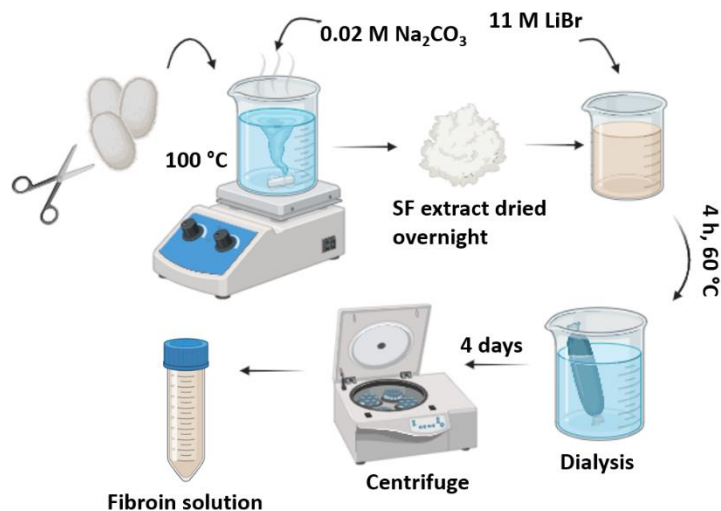


Figure 3.2. Extraction steps of SF from cocoons.

3.4. Production of Calcium- and Strontium-Doped Glass Particles

Two solutions were prepared to start the synthesis of calcium- and strontium-doped glass particles (GPs). For the production of GPs, firstly, an alkaline solution was prepared with distilled water (DI), ethanol (EtOH) and ammonia. Simultaneously, a second solution was also prepared using TEOS as Si source and EtOH. Prepared solutions were stirred separately on magnetic stirrer for 30 min at 600 rpm. Then, second solution was added to the first solution for initiating silica nucleation and stirred for 1 h. Next, 0.90 gram of calcium nitrate (CaN) was added as calcium source. After another 30 min of stirring, 0.48 gram of strontium nitrate (SrN) was added as Sr source and stirring continued for 30 min. At the end of this process, GPs were obtained by centrifuging three times with DI and one time with EtOH to separate and wash the particles from unreacted excess chemicals. Afterwards, particles were dispersed in DI and frozen at 4 °C. Frozen particles were lyophilized for 22 h. Finally, following the drying process, prepared GPs were calcinated for 2 h at 700 °C. GPs was stored in a closed tube until they were used.

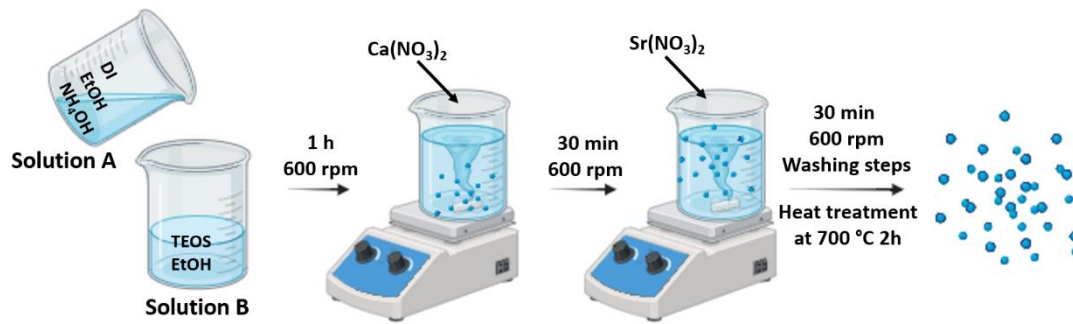


Figure 3.3. Fabrication of GPs via the Stober method.

3.5. Fabrication of the Bilayered DBM

For the bone regeneration side of the membrane (BRS), 10.5 ml of SS solution was transferred into a beaker. 322 μ l glycerol solution was added to SS (30% (w/w) with respect to total polymer content) for the plasticizing effect and started to be stirred at 300 rpm. Stirring process was continued nonstop until the final mixture was poured into petri dish with 90 mm diameter. Simultaneously, GPs were weighted to be 10% (w/w) of the total polymer amount, transferred into a beaker containing 5 ml of DI and placed in ultrasonicator to disperse for 30 min. Thereafter, GPs were added to SS/glycerol mixture under stirring. 2.4 ml of SF solution was also added to the mixture. Lastly, 127 μ l ethanol was added for the crystallization of SF. After mixing these components, the final mixture was placed in a sonicator for 2 min, and then poured into a petri dish. The petri dish was placed in a fume hood at room temperature for 1 day to dry and form a film. Final polymer ratios of the dried film was 70% (w/w) SS and 30% (w/w) SF.

For the soft tissue side of the membrane (STS) that will interact with the soft epithelium tissue, similar steps were repeated. Unlike the first layer, 8.3 ml SS and 6 ml SF solution were used while fabricating this layer and final polymer ratios were adjusted to be 40% (w/w) SS and 60% (w/w) SF. At the end of the mixing process and ultrasonication of all components, the final mixture was poured onto the dried BRS layer in the same petri dish and dried with following the same procedure.

By fabricating and combining these two layers with solvent casting and evaporation method as described above, the flexible bilayered SS/SF/GP composite membranes were fabricated for further experiments.

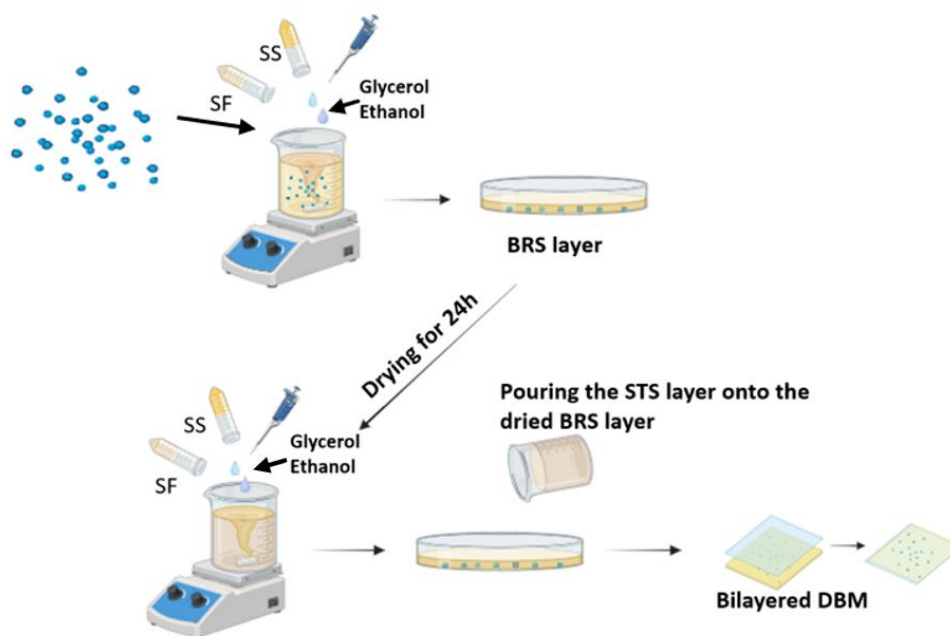


Figure 3.4. Fabrication steps of the bilayered DBM.

3.6. Characterization of the DBM

3.6.1. Scanning Electron Microscopy (SEM)

Morphologies of the GPs, as well as the surface and cross-sections of the produced membranes were examined using FEI Nova Nano SEM 430 SEM with 10 kV accelerating voltage. Prior to imaging, samples were coated with a thin layer of gold to create an electrically conductive path which is a necessary process to achieve SEM imaging of non-conductive materials. Coating process was achieved using Quorum SC7640 sputter coater for 3 min.

3.6.2. Atomic Force Microscopy (AFM)

For surface roughness measurements of the DBMs, Veeco MultiMode AFM was used. Samples were analyzed under ambient condition with tapping mode. A

silicon scanning probe PointProbe-Plus, Nanosensors with tip apex cone angle of 10° and radius smaller than 7 nm was used. 1 μm × 1 μm fields from 3 different regions of samples were analyzed and average root-mean-square (rms) roughness values were reported.

2.6.3. X-Ray Diffraction (XRD)

To characterize the structure of the GPs and membranes, XRD analyses were conducted. Rigaku D/Max - 2200 X-Ray diffractometer was used with monochromatic Cu Kα radiation ($\lambda=1.54 \text{ \AA}$) at 2 °/min scanning rate from 5° to 80° diffraction angles (2θ).

3.6.4. Fourier Transform Infrared Spectroscopy (FTIR)

To evaluate the molecular bonding characteristics of GPs and the membrane, Perkin Elmer 400 spectrometer was used within 4000 and 400 cm⁻¹ region and 4 cm⁻¹ using attenuated total reflection (ATR) configuration. Amid I and amid II regions were evaluated to assess the secondary structure of the membranes.

2.6.5. Inductively Coupled Plasma - Optical Emission Spectrometry (ICP-OES)

ICP-OES analyses were performed to report the elements found in the fabricated GPs and to assess their compositions. Perkin Elmer Optima 4300DV device was used for the measurements.

3.6.6. Water Contact Angle Measurement

Wettability of the surfaces of the bilayered membrane with and without GPs were evaluated with sessile drop water contact angle measurements using Attension Theta equipment. The contact angles of 7 μL distilled water droplets were measured 5 seconds after they were introduced onto the surfaces. The results were obtained from 3 different measurements from each sample.

3.6.7. Degradation and Swelling Tests of the DBM

Samples were prepared by cutting the films into 1 x 1 cm² pieces. Initial weights of the samples were measured. Then, they were placed in 1X Phosphate Buffer Saline (1X PBS) solution (pH 7.4) containing 2% (v/v) penicillin-streptomycin to decrease the risk of contamination. The samples were incubated in 1X PBS for 2 weeks. At specific time intervals, samples were collected from the buffer solutions, weighted and dried. Their final weights were also measured in both wet and dry state to calculate swelling and weight loss behavior of the samples respectively, using the equations below, where W_i is the initial weight, W_f is the final weight and W_w is the wet state weight.

$$Mass\ Loss\% = \left(\frac{W_i - W_f}{W_i} \right) \times 100$$

$$Swelling\% = \left(\frac{W_w - W_i}{W_i} \right) \times 100$$

3.6.8. Mechanical Properties

Uniaxial tensile tests for the bilayered membrane and its layers were conducted using Instron 5565A testing machine. 1 x 5 cm² sheets were cut from films for testing. Gauge length was adjusted to 2 cm and 0.1 mm/s loading rate was applied using a 5 kN load cell. 3 experiments were conducted for each sample group and all samples were tested in wet condition.

3.7. Biological Experiments

3.7.1. Fibroblast Cell Culture and Cytotoxicity Evaluation

To examine the cytotoxicity of the membrane *in vitro*, metabolic activity of cells interacted with the DBM were evaluated. L929 fibroblast cells were cultured using growth medium consisting of DMEM supplemented with 10% (v/v) FBS and 1% (v/v) penicillin-streptomycin under standard cell culture condition (5% CO₂

at 37 °C). Prior to experiments, samples were sterilized with 70% ethanol and UV radiation, each side for 30 min. Afterwards, samples were transferred into tubes containing DMEM and kept at 37 °C for 3 days to obtain the extracts of the samples with a concentration 10 mg/ml. L929 cells were seeded to 96 well plates at a density of 10.000 cells/cm² and cultured for 24 hours in a humidified environment. Then, the media that contains extracts of the samples were added onto the cells and incubated up to 5 days. To investigate cytotoxicity, 3-(4,5-dimethyl-2-thiazolyl)-2,5-diphenyl-2H-tetrazolium bromide (MTT) assay was conducted. After culturing the cells with the extracts for 1, 3 and 5 days culture media were aspirated and cells were rinsed with 1xPBS. 100 µl of 1 mg/ml MTT solution was added to each well and cells were further incubated with the MTT solution for the formation of formazan crystals by viable cells. After 4 hours, 100 µl of 2-propanol/HCL solution was added to dissolve formazan crystals. 100 µl of the resultant solution from each well was transferred to separate wells. Optical density values of wells were measured at 570 nm using Thermo Scientific Multiskan GO spectrophotometer. Experiments were repeated three times.

3.7.2 Preosteoblast Cell Culture and Evaluation of Proliferation

MC3T3-E1 preosteoblast cells were used to examine cellular proliferation and determine the effect of incorporated GPs on cells. Cells were cultured in MEM α supplemented with 10% FBS, 1% penicillin-streptomycin and 1% L-glutamine under standart cell culture conditions (5% CO₂ and 37 °C). Prior to the experiments, previously described protocol was applied for sterilization of the samples (DBMs with and without GPs). MTT assay was conducted as explained previously to evaluate the proliferation of the MC3T3-E1 cells upon their direct interactions with the samples. Cells were seeded at a cell density of 1x10³ cells/cm² onto the samples. Cells were incubated with the samples up to 7 days in vitro. At the 1st, 3rd and 7th days of culture, media were aspirated and samples were rinsed with 1X PBS. Afterwards, samples were transferred into fresh wells and 700 µl of 1 mg/mL MTT solution was added. After 4 hours of incubation, formazan crystals were dissolved by adding 700 µl 2-propanol/HCL solution to each well. 100 µl of

solution with dissolved formazan crystals was transferred from each well to fresh 96 well-plate. Absorbance values were obtained using Thermo Scientific Multiskan GO microplate reader at 570 nm. Experiments were repeated three times with 3 samples.

3.7.3. Morphologies of MC3T3-E1 Preosteoblast Cells

SEM images of MC3T3-E1 preosteoblast cells were obtained after interaction with samples for 3 days to assess cellular morphologies. After sterilization of the samples, cells were seeded on the samples at a density of 5.000 cells/cm² and incubated for 3 days in culture media under standart culture condition. Thereafter, media were aspirated and samples were rinsed with 1X PBS. Cell fixation protocol was applied to achieve SEM imaging. First, cells were treated with paraformaldehyde solution (PFA) for 20 min. After rinsing with 1X PBS, 30%, 50%, 70%, 90%, 95%, 2x100% (v/v) ethanol solutions were added on the cells, respectively. Lastly, hexamethyldisilazane (HMDS) was added and allowed to evaporate at room temperature for final drying of the cells. Prior to imaging, samples containing cells were coated with a thin layer of gold using high resolution sputter coater for 3 min to produce an electrically conductive path.

3.8. Statistical Analysis

Experiments were performed at least three times and results were indicated as mean \pm standart deviation (SD). Statistical analyses were conducted with one way analysis of variance (ANOVA) using Tukey's post hoc test in SPSS software with significance based on $p < 0.05$.

CHAPTER 4

RESULTS AND DISCUSSION

4.1. Characterization of the Fabricated GPs

The synthesized GPs had a spherical shape with a particle size of 351 ± 33 nm, as shown in Figure 4.1a.

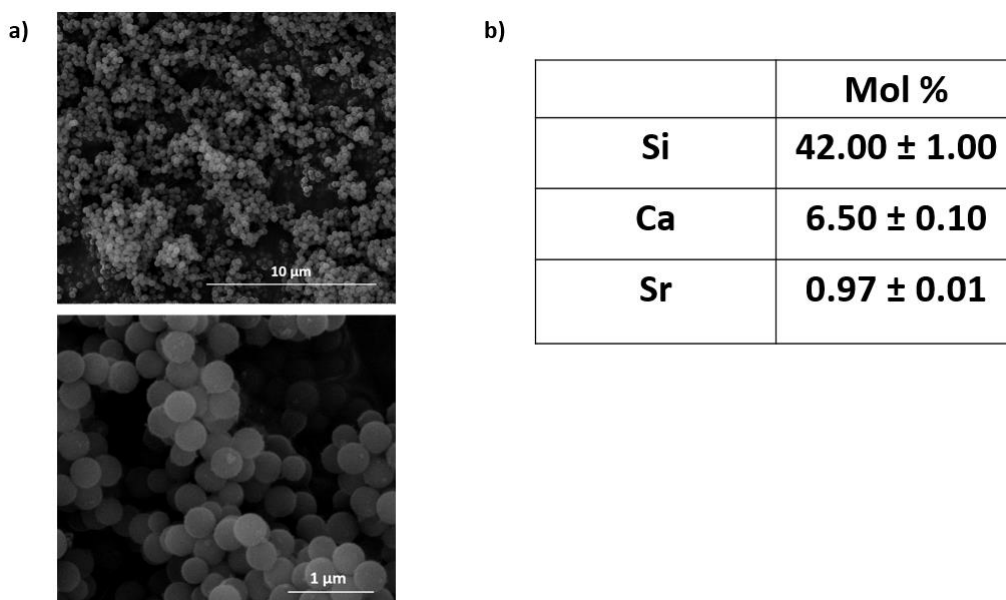


Figure 4.1. (a) SEM images and (b) ICP-OES results showing the composition of the GPs.

OES results indicated the chemical composition of the GPs. Incorporation of the dopant elements with molar ratios of approximately 1% Sr and 6.5% Ca was accomplished, as given in Figure 4.1b.

XRD data obtained from GPs showed that the amorphous particles were synthesized successfully, as shown in Figure 4.2. A broad amorphous peak between 20° and 30° was obtained which is the characteristic peak for the GPs.

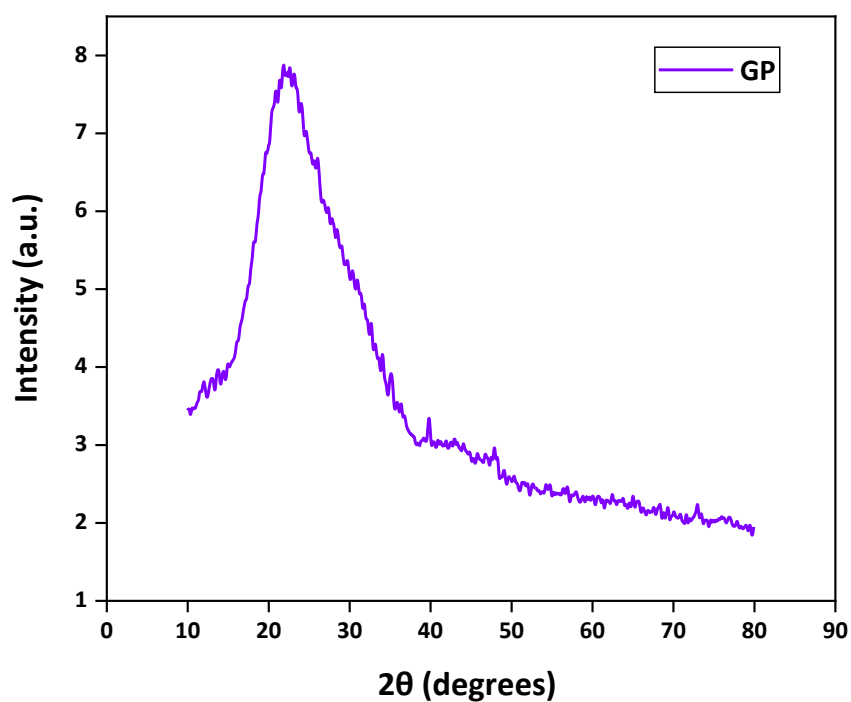


Figure 4.2. XRD spectrum of the fabricated GPs.

Also, the FTIR analyses confirmed the successful fabrication of the GPs. Characteristic bands for GPs were observed at 1055 cm^{-1} and 800 cm^{-1} corresponding to asymmetric stretching vibration of Si-O-Si and symmetric stretching vibration of Si-O-Si, respectively (Barrioni et al., 2019).

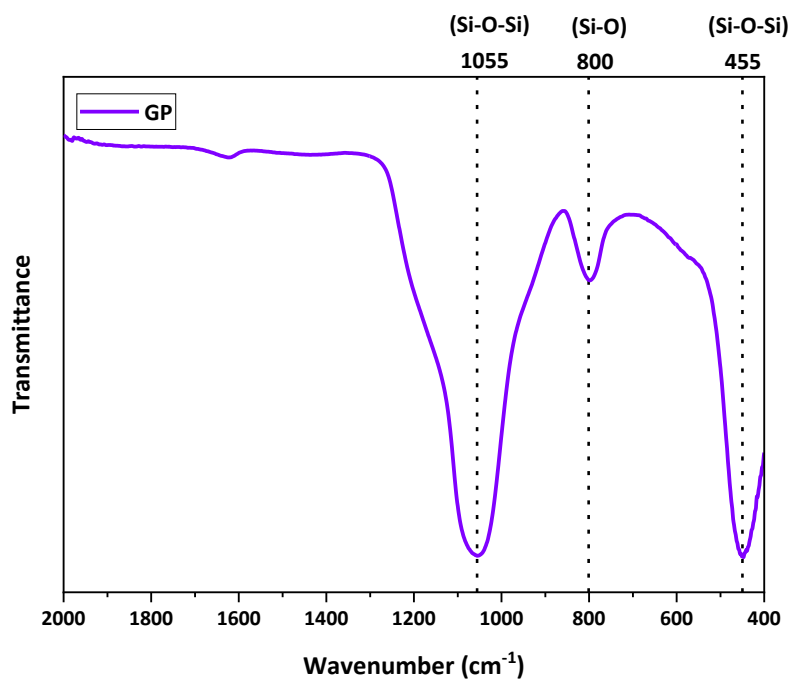


Figure 4.3. FTIR spectrum of the fabricated GPs.

4.2. Characterization of the Fabricated DBM

The bilayered DBM was fabricated with enhanced flexibility due to the addition of glycerol, consistent with the literature (Wang et al., 2015; Yun et al., 2013), as shown in Figure 4.4.

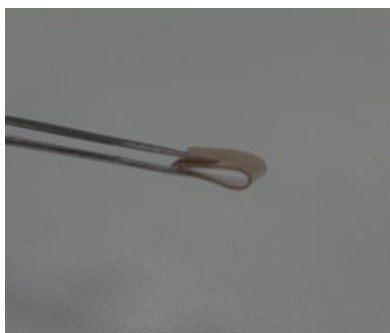


Figure 4.4. Flexibility of the fabricated DBM.

As shown in Figure 4.5, the peaks at 12.1° , 19.9° and 28.2° indicated the Silk II structure in the membranes, which primarily consists of β -sheet structures. Also, peaks at 24.1° and 28.2° indicated the Silk I structure, which mainly contains random coils and α -helices. This data revealed that both β -sheet, α -helix and random coil structures are present in the produced films, as expected (Li et al., 2022). The increase in the peak intensity at 19.9° in STS may indicated an enhancement of the silk II structure, which exhibits a beta-sheet configuration and crystallinity, due to the increased tendency of SF to form β -sheet structures when combined with SS. SS retains more water owing to its water retention capacity and prolongs the drying process of the STS layer compared to the BRS. This results in increased interaction between the polymer chains, water and ethanol, thus enhances the crystallinity (Jaramillo-Quiceno et al., 2024; Puerta et al., 2019). However, further detailed analyses are required to reach a more conclusive result.

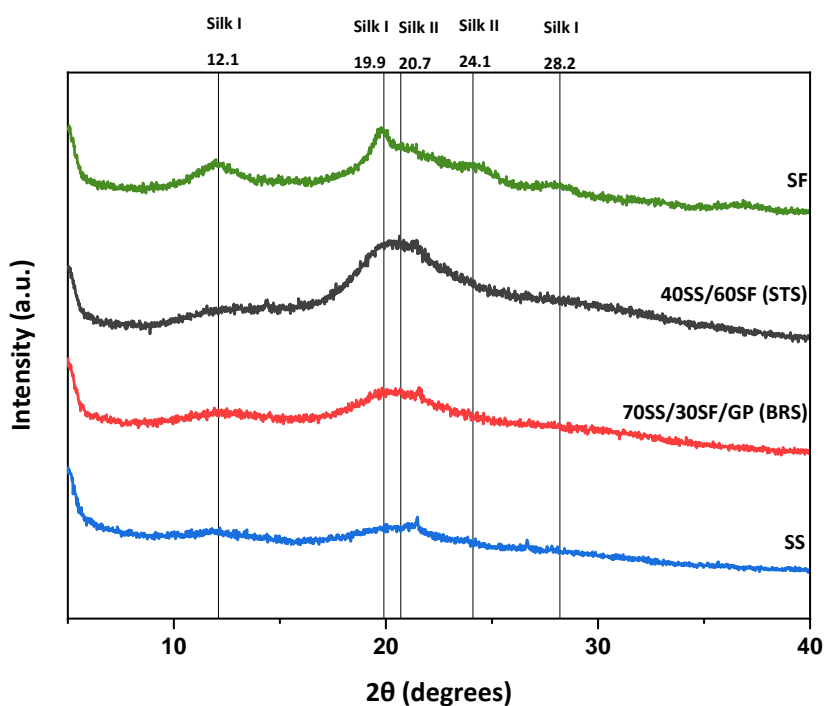


Figure 4.5. XRD spectra of pure SF, STS and BRS layers of the DBM, and pure SS.

All of the films showed peaks at 1118 (C-O) and 995 cm^{-1} (C=C), indicating the presence of glycerol in the films, as shown in Figure 4.6 (Zhang et al., 2011). Bands at 1624 and 1516 cm^{-1} represented Silk II structure containing β -sheets. Additionally, bands at 1650 cm^{-1} indicated Silk I structure (Tiyaboonchai et al., 2011). The presence of these peaks were in-line with the XRD data. The peak at 1650 cm^{-1} became more evident as the SF content increased. This showed the increase of more disorganized structures such as random coils which are prone to form β -sheet structures. To prevent diffusion of glycerol out of the fabricated membranes, ethanol treatment could be applied in low concentrations. Due to the low amount and duration of the ethanol treatment for the crystallization of SF, a significant amount of disorganized structure lacking the beta-sheet configuration remained.

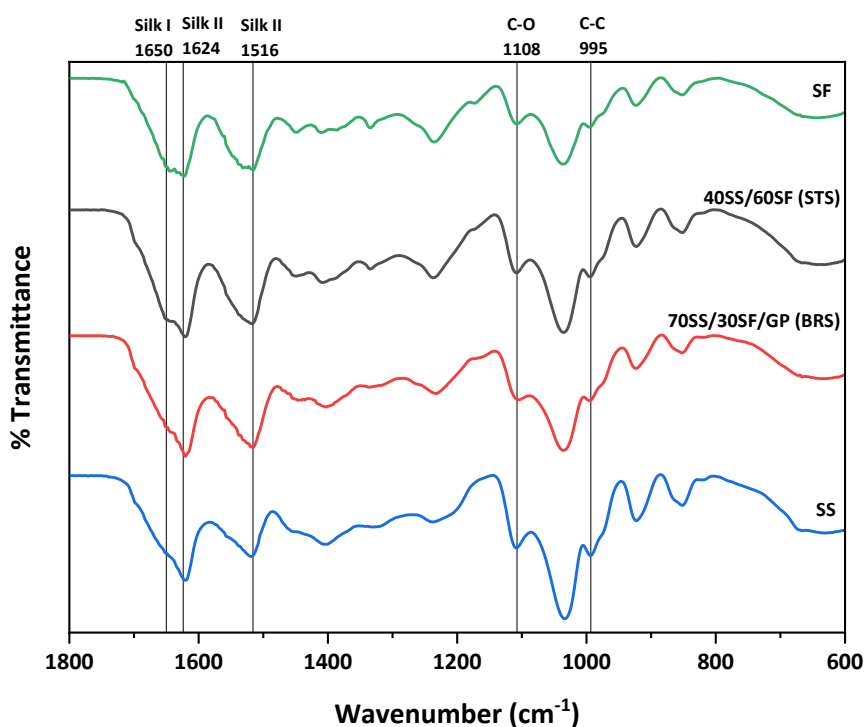


Figure 4.6. FTIR spectra of pure SF, STS and BRS layers of the DBM, and pure SS.

SEM images of the surfaces of the DBM demonstrated that the addition of GPs created a rough surface topography. The BRS layer which will face the bone regeneration area showed nano structured roughness. On the other hand, the STS layer which will interact with the soft tissue did not contain GPs and showed a much smoother surface, as shown in Figure 4.7.

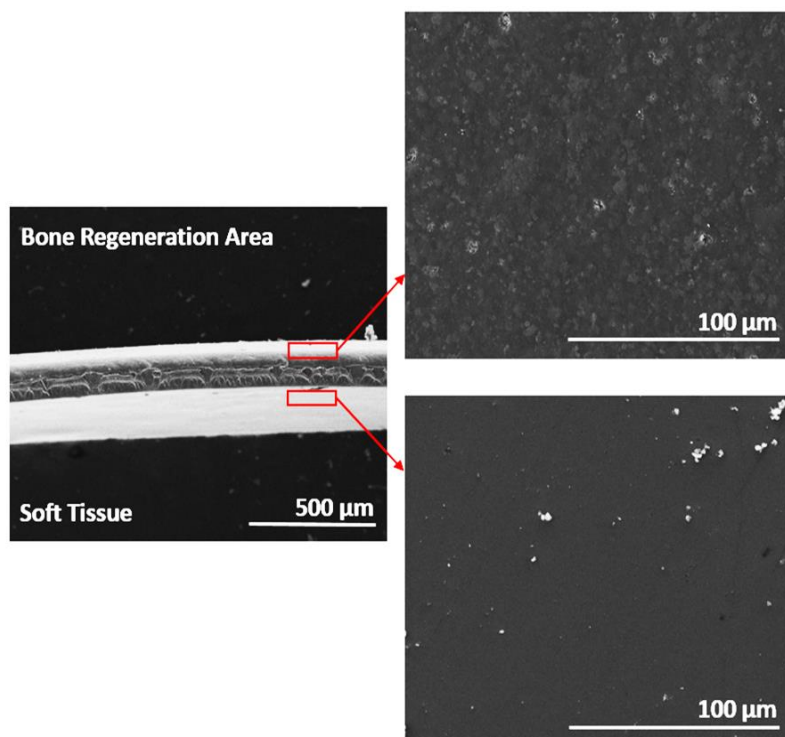


Figure 4.7. SEM images of the cross-section of the DBM (left), and top surfaces of the BRS and STS layers of the DBM.

AFM results supported the SEM images and confirmed the nanostructured roughness on the surface of the BRS, as represented in Figure 4.8a. The RMS value of the BRS was measured as 24.6 nm and found to be significantly higher than that of STS, which was 16.7 nm, as shown in Figure 4.8b.

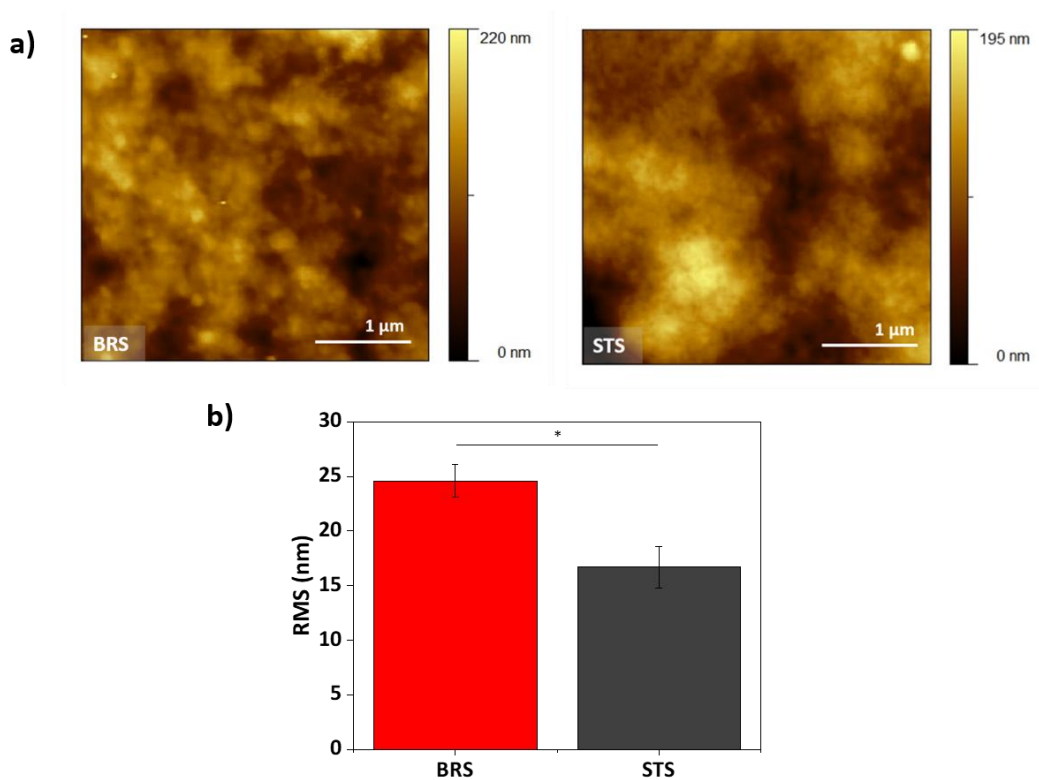


Figure 4.8. (a) AFM images of BRS (left) and STS (right), and (b) graph indicating the RMS values of BRS and STS. * $p < 0.05$.

The SS films exhibited rapid swelling, as indicated in the literature (He et al., 2017; Munir et al., 2023). As shown in Figure 4.9, BRS showed the highest swelling ratio due to the hydrophilic nature of SS. Also, it was obtained that incorporation of GPs into 70SS/30SF films further enhanced the swelling ratio of the films because of the hydrophilicity of the GPs (Cao & Zhang, 2016; K. Huang et al., 2014). Pure SF film showed the lowest swelling as a result of its hydrophobicity and more compact structure in β -sheet crystallines of SF (Jameson et al., 2021).

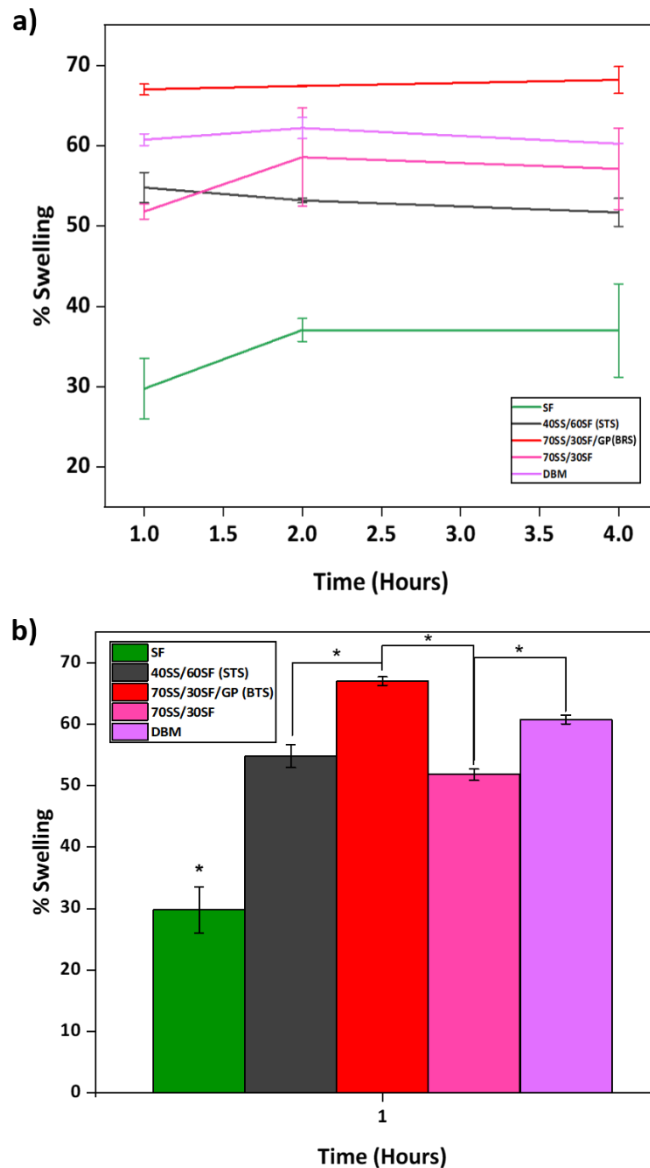


Figure 4.9. % Swelling values of SF, STS, BRS, 70SS/30SF and DBM samples in 1x PBS upon 4 h of immersion time. Values are mean \pm SD (n=3), *p< 0.05.

Degradation tests were conducted for two weeks to evaluate the % weight loss from the samples. Degradation rate is an important parameter for an absorbable DBM and should match with the healing rate of the bone. Additionally, the DBM should preserve its integrity to function as barrier until the treatment ends (Rider et al., 2022).

The BRS exhibited the highest mass loss which was about 40% of its initial mass, as shown in Figure 4.10. This result can also be explained with the high hydrophilicity of sericin, and further improvement of the hydrophilicity by the addition of GPs (Ekasurya et al., 2023; Vukajlovic et al., 2019). However, the majority of the mass loss from the samples was due to the glycerol elimination from the samples which was approximately 25-30% at the end of the 1st day. Thus, the rapid decrease of weight in all samples was a result of glycerol diffusion out off the films within a short period of time. After the 1st day, the BRS still had the highest weight loss which was approximately 52%, including the weight loss resulted from glycerol. The STS was expected to degrade slower compared to BRS, and showed lower weight loss which was nearly 43% of its initial weight.

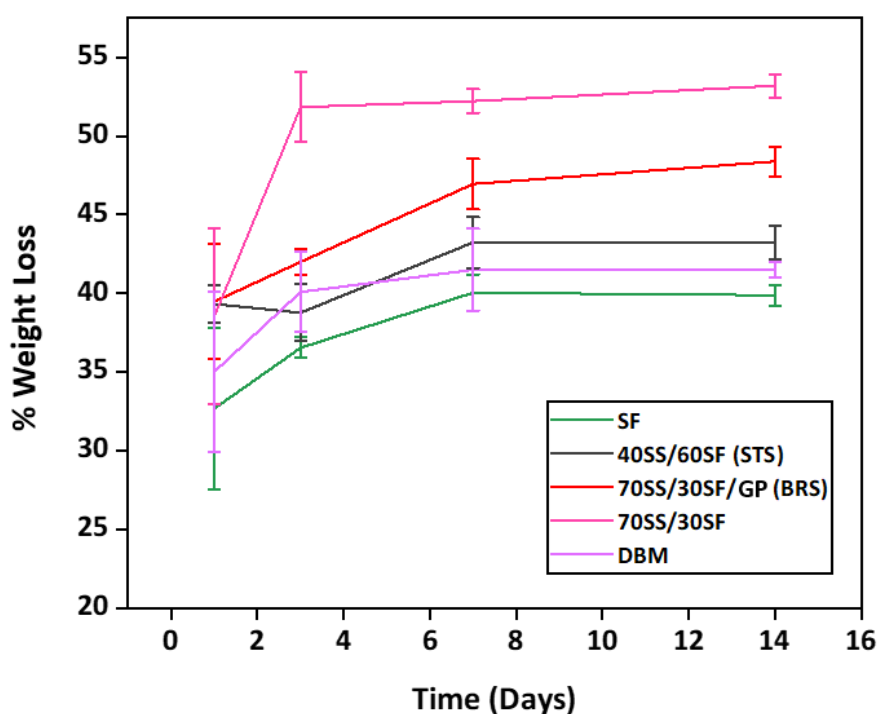


Figure 4.10. % Weight loss for pure SF, STS, BRS, 70SS/30SF and DBM samples in 1x PBS up to 2 weeks.

Water contact angle results proved the improvement of the hydrophilicity when the SS ratio was increased in the membrane, as shown in Table 4.1. However, despite

the hydrophilic nature of GPs, they did not significantly effect the water contact angle. This could be attributed to the embedment of GPs into the polymer which may have prevented the GPs from altering the surface chemistry of the membrane. Additionally, nanostructured roughness on the surface of the BRS might have also influenced this outcome.

Table 4.1. Sessile drop water contact angle results of the samples.

	Water Contact Angle
70SS/30SF/BG (BRS)	78.9 ± 1.2
70SS/30SF	80.6 ± 2.8
40SS/60SF (STS)	101.9 ± 2.5

Mechanical strength of DBMs should be sufficient to resist the pressure of the soft tissue. When the BRS and STS layers of the bilayered DBM was compared, significant difference could observed, as illustrated in Figure 4.9. BRS was expected to show lower modulus compared to STS because of its higher SS content, which is a naturally weak material. However, the incorporation of GPs might have improved the mechanical properties of the BRS. DBM showed the highest modulus which was approximately 11 MPa suitable for absorbable DBM applications (Wang et al., 2023). This may be a result of the fabrication process of the bilayered membrane. After the first layer was poured into petri dish and dried, the second layer that contains ethanol and water was poured onto the first layer. This process might have resulted in further crystallization of the bottom layer and leads to DBM having higher modulus.

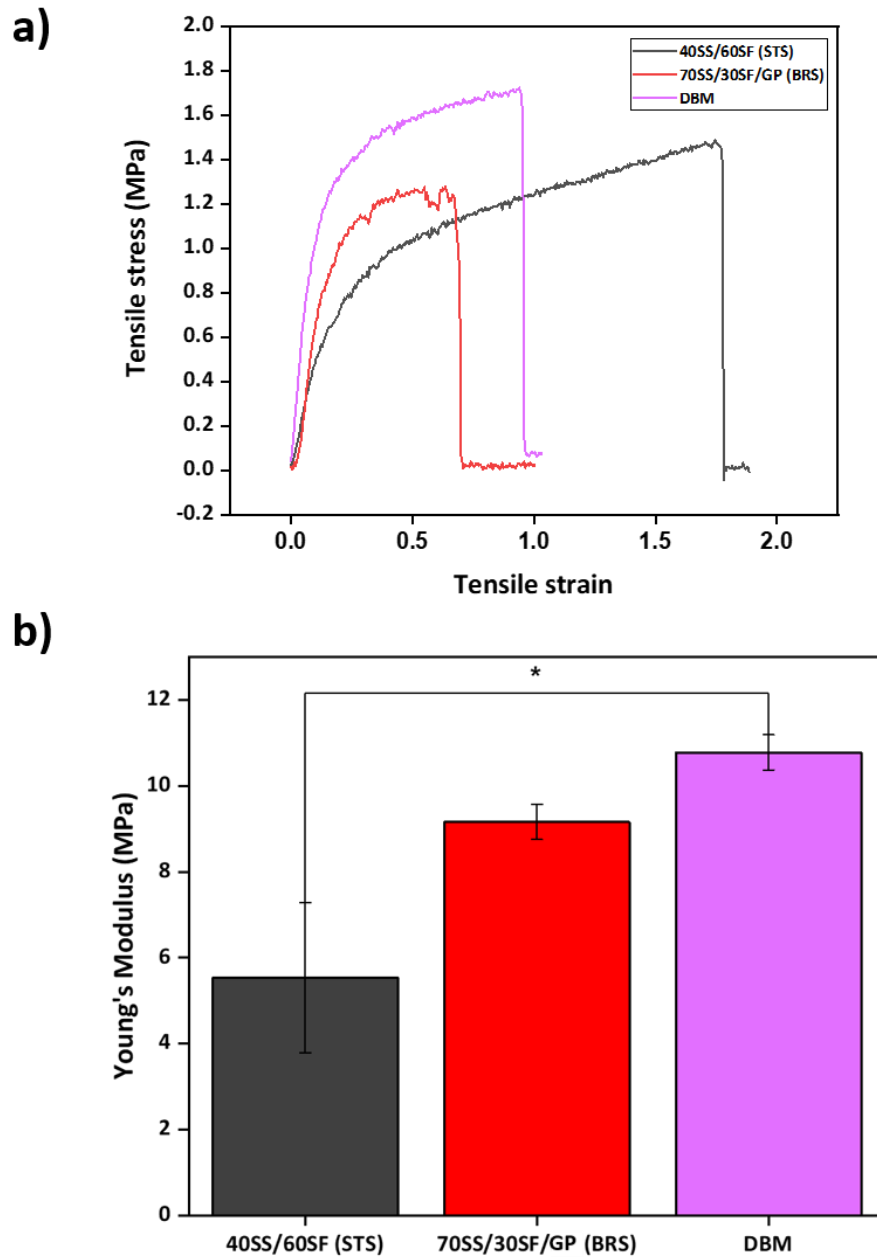


Figure 4.11. (a) Stress-strain graphs and (b) Young's modulus values of the STS, BRS and DBM samples calculated from the elastic region of the stress-strain graph. Values are mean \pm SD (n=3), *p< 0.05.

4.3. Biological Evaluation of the DBM

4.3.1. Cytotoxicity Evaluation of the DBM

The bilayered DBM did not show any cytotoxic effects on L919 fibroblast cells, as represented in Figure 4.10. There were no statistically significant differences between the DBM and control samples at the 1st and 3rd days of culture. However, on the 5th day of culture, the control group (tissue culture polystyrene) exhibited higher cell density compared to DBM.

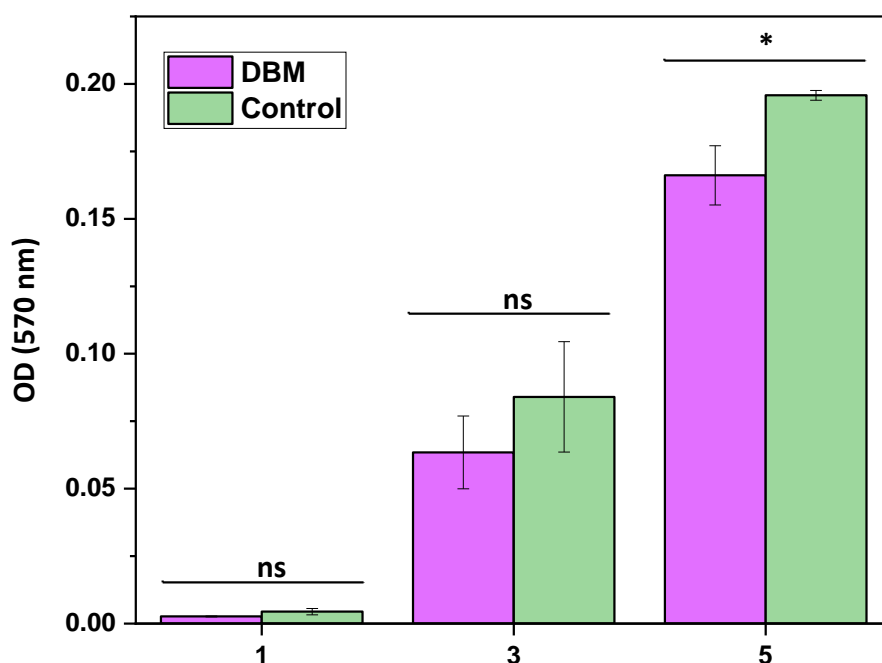


Figure 4.12. Viability of L929 fibroblasts up to 5 days in vitro. Cells were incubated with the extract of the DBM. Values are mean \pm SD, n=3. *p < 0.05, ns: non-significant.

4.3.2. MC3T3-E1 Preosteoblast Cell Proliferation

The results of the MTT assay conducted to examine the effects of GPs on MC3T3-E1 preosteoblast cells. There were no statistically significant differences between the DBM with or without GPs on the 1st and 3rd days of culture. However, there was a significant difference at 7th day of the culture between the sample groups, as shown in Figure 4.11.

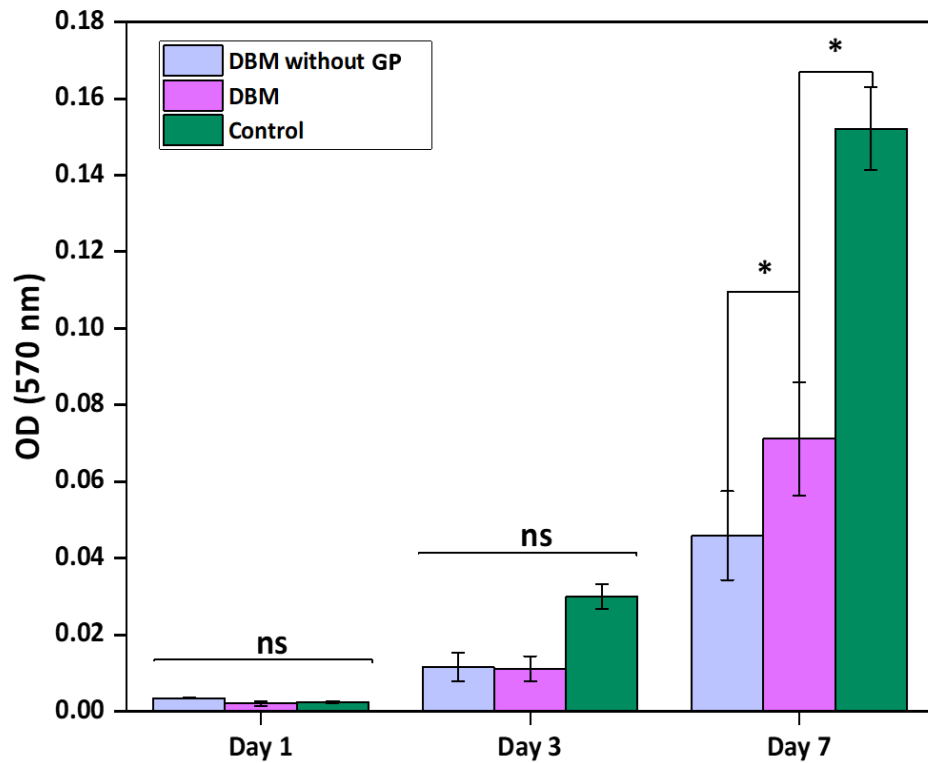


Figure 4.13. Proliferation of MCT3-E1 preosteoblasts up to 7 days in vitro. Cells were seeded directly on the DBM. Values are mean \pm SD, n=3. *p< 0.05, ns: non-significant.

This was possibly due to the ions released from GPs, such as strontium, calcium or silicium (Polo-Montalvo et al., 2021). Also, the nanostructured roughness on the surface of the BRS might have effected the proliferation of the cells (Vandrovcova et al., 2012), as shown in Figure 4.12.

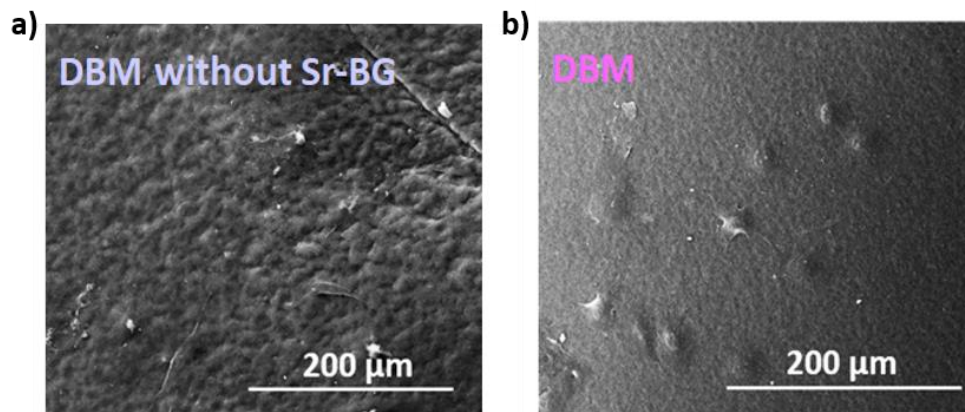


Figure 4.14. Attached cells on the membrane (a) without and (b) with GPs, respectively

The fabricated bilayered DBM was tested in this thesis to evaluate if the designed composition was suitable for DBM applications.

In absorbable DBM applications, matching of the degradation rate of DBM and the regeneration of the bone is crucial in order for the membrane to fulfill its intended function effectively (Rider et al., 2022). In this study, SS and SF were blended in specific ratios to achieve optimal degradation rates for each layer. As evaluated from the results, the BRS layer degraded faster than the STS layer due to its high SS ratio and hydrophilic nature of SS (Duan et al., 2016). Since the hydrophilicity increases as the SS content increases as confirmed by the swelling and water contact angle results, the degradation rate was measured higher in the BRS layer than the STS layer. Additionally, the incorporation of hydrophilic GPs further enhanced the hydrophilicity of the BRS layer, compatible with literature (Boccaccini et al., 2010). The quicker degradation of the BRS layer was desired to facilitate earlier interaction of the GPs with the biological environment. The STS layer with a higher SF content exhibited the lowest degradation rate after pure SF, which can be attributed to more hydrophobic nature of SF compared to SS (Matsumoto et al., 2006). On the other hand, the STS layer, with its slower degradation rate, ensures that the membrane maintains its barrier function throughout the treatment period, thus effectively serving its intended function.

In addition, the mechanical properties of the membrane must be sufficient to withstand the pressure of the soft tissue, which grows faster than the bone tissue. According to the tensile test results, the membrane's Young's modulus was calculated to be approximately 11 MPa, which is adequate for DBM applications (M. Y. Lee et al., 2024). Contrary to expectations, the BRS layer with high SS content was calculated to have a higher modulus, compared to the STS layer containing higher SF content which is a mechanically stronger material. This may be due to the reinforcement effect created by the incorporation of GPs which improved the mechanical properties. Additionally, the water retention capacity of the BRS layer was higher due to its SS ratio (Lee et al., 2023). This resulted in a longer drying time and consequently a longer crystallization period. Moreover, despite all the samples were produced in the same thickness, the modulus of the DBM was measured to be higher than that of both layers. This may be due to the fabrication steps of the DBM. After the first layer was cast and dried, the addition of the second layer caused extra crystallization on the first cast layer so the modulus of the final version of the DBM became higher than its separate layers.

The biological properties of the DBM also play an important role for enhancing the effectiveness of the treatment (Leal et al., 2013). GPs were incorporated to enhance the biological properties of the designed DBM for supporting bone regeneration. From the results of the experiments conducted with preosteoblasts, it was demonstrated that the addition of GPs to the BRS layer improved cell proliferation and cell spreading, due to the ions released from the GPs and the created nanostructured surface roughness (Sergi et al., 2020).

CHAPTER 5

CONCLUSION

In this study, SS and SF solutions were fabricated successfully as well as Ca- and Sr-doped GPs. In addition, the DBM was fabricated to have a bilayered structure where soft tissue side was fibroin rich and bone tissue side was sericin rich. Glycerol was also incorporated to enhance the flexibility of the fabricated DBMs. XRD and FTIR results confirmed successful blending of SS and SF in the films. GPs enhanced the nanostructured roughness of BRS layer of the DBM from approximately from 17 nm to 25 nm. The BRS layer without the GPs showed the highest degradation rate due to its high SS ratio. In addition, the BRS layer exhibited the highest swelling ratio due to its improved hydrophilicity due to the incorporation of GPs and high SS ratio. Young's modulus of the DBM was evaluated to be nearly 11 MPa, which was adequate for DBM applications. Incorporation of GPs did not create cytotoxicity and improved bone cell proliferation up to 7 days in vitro.

This thesis offered an alternative application area for silk sericin and fibroin blends in the biomaterials field. Results cumulatively indicated that the designed membrane is promising for DBM applications and require further investigation.

CHAPTER 6

FUTURE WORK

Although this work showed that the designed bilayered dental barrier membrane can be a suitable material for guided tissue regeneration applications, various aspects need to be further investigated:

- More detailed analyses of the FTIR and XRD patterns to evaluate the β -sheet content of SS and SF.
- Osteoblast cellular functions (ALP, Ca deposition).
- Dual doping of the glass nanoparticles (i.e. Ag, Cu) to impart antibacterial properties to the designed membrane.
- Weight loss behavior at different pH values with and without an enzyme.

REFERENCES

- Al-Harbi, N., Mohammed, H., Al-Hadeethi, Y., Bakry, A. S., Umar, A., Hussein, M. A., Abbassy, M. A., Vaidya, K. G., Al Berakdar, G., Mkawi, E. M., & Nune, M. (2021). Silica-based bioactive glasses and their applications in hard tissue regeneration: A review. In *Pharmaceuticals*. <https://doi.org/10.3390/ph14020075>
- Alqahtani, A. M. (2023). Guided Tissue and Bone Regeneration Membranes: A Review of Biomaterials and Techniques for Periodontal Treatments. In *Polymers*. <https://doi.org/10.3390/polym15163355>
- Aramwit, P., Siritientong, T., & Srichana, T. (2012). Potential applications of silk sericin, a natural protein from textile industry by-products. In *Waste Management and Research*. <https://doi.org/10.1177/0734242X11404733>
- Asakura, T., & Williamson, M. P. (2023). A review on the structure of Bombyx mori silk fibroin fiber studied using solid-state NMR: An antipolar lamella with an 8-residue repeat. In *International Journal of Biological Macromolecules*. <https://doi.org/10.1016/j.ijbiomac.2023.125537>
- Assadi, Z., Rezvanian, P., Gounani, Z., Ejeian, F., Zarrabi, A., & Masaeli, E. (2024). Multilayered nanocomposite membrane orchestrating targeted dual release strategies for enhanced guided bone regeneration. *Chemical Engineering Journal*. <https://doi.org/10.1016/j.cej.2024.149237>
- Babu, P. J., & Suamte, L. (2024). Applications of silk-based biomaterials in biomedicine and biotechnology. In *Engineered Regeneration*. <https://doi.org/10.1016/j.engreg.2023.11.002>
- Barreto, M. E. V., Medeiros, R. P., Shearer, A., Fook, M. V. L., Montazerian, M., & Mauro, J. C. (2023). Gelatin and Bioactive Glass Composites for Tissue Engineering: A Review. In *Journal of Functional Biomaterials*. <https://doi.org/10.3390/jfb14010023>

- Barrioni, B. R., Norris, E., Li, S., Naruphontjirakul, P., Jones, J. R., & Pereira, M. de M. (2019). Osteogenic potential of sol–gel bioactive glasses containing manganese. *Journal of Materials Science: Materials in Medicine*. <https://doi.org/10.1007/s10856-019-6288-9>
- Bee, S. L., & Hamid, Z. A. A. (2022). Asymmetric resorbable-based dental barrier membrane for periodontal guided tissue regeneration and guided bone regeneration: A review. In *Journal of Biomedical Materials Research - Part B Applied Biomaterials*. <https://doi.org/10.1002/jbm.b.35060>
- Boccaccini, A. R., Erol, M., Stark, W. J., Mohn, D., Hong, Z., & Mano, J. F. (2010). Polymer/bioactive glass nanocomposites for biomedical applications: A review. *Composites Science and Technology*. <https://doi.org/10.1016/j.compscitech.2010.06.002>
- Brown, J. E., Davidowski, S. K., Xu, D., Cebe, P., Onofrei, D., Holland, G. P., & Kaplan, D. L. (2016). Thermal and Structural Properties of Silk Biomaterials Plasticized by Glycerol. *Biomacromolecules*. <https://doi.org/10.1021/acs.biomac.6b01260>
- Caballé-Serrano, J., Sawada, K., Miron, R. J., Bosshardt, D. D., Buser, D., & Gruber, R. (2017). Collagen barrier membranes adsorb growth factors liberated from autogenous bone chips. *Clinical Oral Implants Research*. <https://doi.org/10.1111/clr.12789>
- Cao, T. T., & Zhang, Y. Q. (2016). Processing and characterization of silk sericin from *Bombyx mori* and its application in biomaterials and biomedicines. In *Materials Science and Engineering C*. <https://doi.org/10.1016/j.msec.2015.12.082>
- Çapar, G., & Aygün, S. S. (2015). Characterization of sericin protein recovered from silk wastewaters. *Türk Hijyen ve Deneysel Biyoloji Dergisi*. <https://doi.org/10.5505/TurkHijyen.2015.47113>

- Carissimi, G., Lozano-Pérez, A. A., Montalbán, M. G., Aznar-Cervantes, S. D., Cenis, J. L., & VÍllora, G. (2019). Revealing the influence of the degumming process in the properties of silk fibroin nanoparticles. *Polymers*. <https://doi.org/10.3390/polym11122045>
- Chirila, T. V., Suzuki, S., & McKirdy, N. C. (2016). Further development of silk sericin as a biomaterial: comparative investigation of the procedures for its isolation from *Bombyx mori* silk cocoons. *Progress in Biomaterials*. <https://doi.org/10.1007/s40204-016-0052-8>
- Dogan, N., Murat Okcu, K., Ortakoglu, K., Dalkiz, M., & Gunaydin, Y. (2003). Barrier membrane and bone graft treatments of dehiscence-type defect at existing implant: A case report. *Implant Dentistry*. <https://doi.org/10.1097/01.ID.0000042505.64374.85>
- dos Santos, F. V., Siqueira, R. L., de Moraes Ramos, L., Yoshioka, S. A., Branciforti, M. C., & Correa, D. S. (2024). Silk fibroin-derived electrospun materials for biomedical applications: A review. In *International Journal of Biological Macromolecules*. <https://doi.org/10.1016/j.ijbiomac.2023.127641>
- Drevet, R., Fauré, J., & Benhayoune, H. (2024). Electrophoretic Deposition of Bioactive Glass Coatings for Bone Implant Applications: A Review. *Coatings*, *14*(9), 1084. <https://doi.org/10.3390/coatings14091084>
- Duan, L., Yuan, J., Yang, X., Cheng, X., & Li, J. (2016). Interaction study of collagen and sericin in blending solution. *International Journal of Biological Macromolecules*. <https://doi.org/10.1016/j.ijbiomac.2016.09.003>
- Ekasurya, W., Sebastian, J., Puspitasari, D., Asri, P. P. P., & Asri, L. A. T. W. (2023). Synthesis and Degradation Properties of Sericin/PVA Hydrogels. *Gels*. <https://doi.org/10.3390/gels9020076>
- Gaviria, A., Jaramillo-Quiceno, N., Motta, A., & Restrepo-Osorio, A. (2023). Silk wastes and autoclaved degumming as an alternative for a sustainable silk process. *Scientific Reports*. <https://doi.org/10.1038/s41598-023-41762-6>

- Gürbüz, S., Demirtaş, T. T., Yüksel, E., Karakeçili, A., Doğan, A., & Gümüşderelioğlu, M. (2016). Multi-layered functional membranes for periodontal regeneration: Preparation and characterization. *Materials Letters*. <https://doi.org/10.1016/j.matlet.2016.05.054>
- He, H., Cai, R., Wang, Y., Tao, G., Guo, P., Zuo, H., Chen, L., Liu, X., Zhao, P., & Xia, Q. (2017). Preparation and characterization of silk sericin/PVA blend film with silver nanoparticles for potential antimicrobial application. *International Journal of Biological Macromolecules*. <https://doi.org/10.1016/j.ijbiomac.2017.06.009>
- Hoornaert, A., D'Arros, C., Heymann, M. F., & Layrolle, P. (2016). Biocompatibility, resorption and biofunctionality of a new synthetic biodegradable membrane for guided bone regeneration. *Biomedical Materials (Bristol)*. <https://doi.org/10.1088/1748-6041/11/4/045012>
- Hu, D., Li, T., Liang, W., Wang, Y., Feng, M., & Sun, J. (2023). Silk sericin as building blocks of bioactive materials for advanced therapeutics. In *Journal of Controlled Release*. <https://doi.org/10.1016/j.jconrel.2022.11.019>
- Huang, K., Cai, S., Xu, G., Ren, M., Wang, X., Zhang, R., Niu, S., & Zhao, H. (2014). Sol-gel derived mesoporous 58S bioactive glass coatings on AZ31 magnesium alloy and in vitro degradation behavior. *Surface and Coatings Technology*. <https://doi.org/10.1016/j.surfcoat.2013.12.026>
- Huang, L., Shi, J., Zhou, W., & Zhang, Q. (2023). Advances in Preparation and Properties of Regenerated Silk Fibroin. In *International Journal of Molecular Sciences*. <https://doi.org/10.3390/ijms241713153>
- Huang, W., Ling, S., Li, C., Omenetto, F. G., & Kaplan, D. L. (2018). Silkworm silk-based materials and devices generated using bio-nanotechnology. In *Chemical Society Reviews*. <https://doi.org/10.1039/c8cs00187a>
- Jameson, J. F., Pacheco, M. O., Butler, J. E., & Stoppel, W. L. (2021). Estimating Kinetic Rate Parameters for Enzymatic Degradation of Lyophilized Silk

Fibroin Sponges. *Frontiers in Bioengineering and Biotechnology*.
<https://doi.org/10.3389/fbioe.2021.664306>

Jaramillo-Quiceno, N., Duque Carmona, A. S., Serna, J. S., Carmona, D. M., Torres-Taborda, M., Hincapié-Llanos, G. A., Marín, J. F. S., & Álvarez-López, C. (2024). Enhancing soil water retention and plant growth with thermal crosslinked silk sericin-based hydrogel. *Journal of Environmental Chemical Engineering*. <https://doi.org/10.1016/j.jece.2024.112260>

Johari, N., Khodaei, A., Samadikuchaksaraei, A., Reis, R. L., Kundu, S. C., & Moroni, L. (2022). Ancient fibrous biomaterials from silkworm protein fibroin and spider silk blends: Biomechanical patterns. In *Acta Biomaterialia*. <https://doi.org/10.1016/j.actbio.2022.09.030>

Kim, K., Su, Y., Kucine, A. J., Cheng, K., & Zhu, D. (2023). Guided Bone Regeneration Using Barrier Membrane in Dental Applications. In *ACS Biomaterials Science and Engineering*. <https://doi.org/10.1021/acsbiomaterials.3c00690>

King, J. A., Zhang, X., & Ries, M. E. (2023). The Formation of All-Silk Composites and Time–Temperature Superposition. In *Materials*. <https://doi.org/10.3390/ma16103804>

Ko, Y. G., Lee, M., Park, W. H., Cho, D., Kwon, O. K., & Kwon, O. H. (2016). Guiding bone regeneration using hydrophobized silk fibroin nanofiber membranes. *Macromolecular Research*. <https://doi.org/10.1007/s13233-016-4109-2>

Koh, L. D., Cheng, Y., Teng, C. P., Khin, Y. W., Loh, X. J., Tee, S. Y., Low, M., Ye, E., Yu, H. D., Zhang, Y. W., & Han, M. Y. (2015). Structures, mechanical properties and applications of silk fibroin materials. In *Progress in Polymer Science*. <https://doi.org/10.1016/j.progpolymsci.2015.02.001>

- Kundu, B., Rajkhowa, R., Kundu, S. C., & Wang, X. (2013). Silk fibroin biomaterials for tissue regenerations. In *Advanced Drug Delivery Reviews*. <https://doi.org/10.1016/j.addr.2012.09.043>
- Leal, A. I., Caridade, S. G., Ma, J., Yu, N., Gomes, M. E., Reis, R. L., Jansen, J. A., Walboomers, X. F., & Mano, J. F. (2013). Asymmetric PDLA membranes containing Bioglass® for guided tissue regeneration: Characterization and in vitro biological behavior. *Dental Materials*. <https://doi.org/10.1016/j.dental.2013.01.009>
- Lee, H. G., Jang, M. J., Park, B. D., & Um, I. C. (2023). Structural Characteristics and Properties of Redissolved Silk Sericin. *Polymers*. <https://doi.org/10.3390/polym15163405>
- Lee, M. Y., Yoon, H. W., Lee, S. Y., Kim, K. M., Shin, S. J., & Kwon, J. S. (2024). Mineral trioxide aggregate in membrane form as a barrier membrane in guided bone regeneration. *Journal of Dental Sciences*. <https://doi.org/10.1016/j.jds.2023.11.021>
- Li, M., Tian, W., Zhang, Y., Song, H., Yu, Y., Chen, X., Yong, N., Li, X., Yin, Y., Fan, Q., & Wang, J. (2022). Enhanced Silk Fibroin/Sericin Composite Film: Preparation, Mechanical Properties and Mineralization Activity. *Polymers*. <https://doi.org/10.3390/polym14122466>
- Liu, J., Shi, L., Deng, Y., Zou, M., Cai, B., Song, Y., Wang, Z., & Wang, L. (2022). Silk sericin-based materials for biomedical applications. In *Biomaterials*. <https://doi.org/10.1016/j.biomaterials.2022.121638>
- Long, Y., Cheng, X., Tang, Q., & Chen, L. (2021). The antigenicity of silk-based biomaterials: sources, influential factors and applications. In *Journal of Materials Chemistry B*. <https://doi.org/10.1039/d1tb00752a>
- Lu, S., Wang, P., Zhang, F., Zhou, X., Zuo, B., You, X., Gao, Y., Liu, H., & Tang, H. (2015). A novel silk fibroin nanofibrous membrane for guided bone

regeneration: A study in rat calvarial defects. *American Journal of Translational Research*.

- Luo, D., Yao, C., Zhang, R., Zhao, R., Iqbal, M. Z., Mushtaq, A., Lee, I. S., & Kong, X. (2021). Silk Fibroin/Collagen Blended Membrane Fabricated via a Green Papermaking Method for Potential Guided Bone Regeneration Application: In Vitro and in Vivo Evaluation. *ACS Biomaterials Science and Engineering*, 7(12), 5788–5797. <https://doi.org/10.1021/acsbmaterials.1c01060>
- Luz, E. P. C. G., das Chagas, B. S., de Almeida, N. T., de Fátima Borges, M., Andrade, F. K., Muniz, C. R., Castro-Silva, I. I., Teixeira, E. H., Popat, K., de Freitas Rosa, M., & Vieira, R. S. (2020). Resorbable bacterial cellulose membranes with strontium release for guided bone regeneration. *Materials Science and Engineering C*. <https://doi.org/10.1016/j.msec.2020.111175>
- Ma, L., Dong, W., Lai, E., & Wang, J. (2024). Silk fibroin-based scaffolds for tissue engineering. *Frontiers in Bioengineering and Biotechnology*, 12(April), 1–15. <https://doi.org/10.3389/fbioe.2024.1381838>
- Matic, T., Daou, F., Cochis, A., Barac, N., Ugrinovic, V., Rimondini, L., & Veljovic, D. (2024). Multifunctional Sr,Mg-Doped Mesoporous Bioactive Glass Nanoparticles for Simultaneous Bone Regeneration and Drug Delivery. *International Journal of Molecular Sciences*, 25(15). <https://doi.org/10.3390/ijms25158066>
- Matsumoto, A., Chen, J., Collette, A. L., Kim, U. J., Altman, G. H., Cebe, P., & Kaplan, D. L. (2006). Mechanisms of silk fibroin sol-gel transitions. *Journal of Physical Chemistry B*. <https://doi.org/10.1021/jp056350v>
- Ming, P., Rao, P., Wu, T., Yang, J., Lu, S., Yang, B., Xiao, J., & Tao, G. (2022). Biomimetic Design and Fabrication of Sericin-Hydroxyapatite Based Membranes With Osteogenic Activity for Periodontal Tissue Regeneration.

Frontiers in Bioengineering and Biotechnology.
<https://doi.org/10.3389/fbioe.2022.899293>

Morin, A., Pahlevan, M., & Alam, P. (2017). Silk biocomposites: Structure and chemistry. In *Handbook of Composites from Renewable Materials*.
<https://doi.org/10.1002/9781119441632.ch8>

Mota, J., Yu, N., Caridade, S. G., Luz, G. M., Gomes, M. E., Reis, R. L., Jansen, J. A., Frank Walboomers, X., & Mano, J. F. (2012). Chitosan/bioactive glass nanoparticle composite membranes for periodontal regeneration. *Acta Biomaterialia*. <https://doi.org/10.1016/j.actbio.2012.06.040>

Mouriño, V., Vidotto, R., Cattalini, J. P., & Boccaccini, A. R. (2019). Enhancing biological activity of bioactive glass scaffolds by inorganic ion delivery for bone tissue engineering. In *Current Opinion in Biomedical Engineering*.
<https://doi.org/10.1016/j.cobme.2019.02.002>

Munir, F., Tahir, H. M., Ali, S., Ali, A., Tehreem, A., Zaidi, S. D. E. S., Adnan, M., & Ijaz, F. (2023). Characterization and Evaluation of Silk Sericin-Based Hydrogel: A Promising Biomaterial for Efficient Healing of Acute Wounds. *ACS Omega*. <https://doi.org/10.1021/acsomega.3c04178>

Nasajpour, A., Ansari, S., Rinoldi, C., Rad, A. S., Aghaloo, T., Shin, S. R., Mishra, Y. K., Adelung, R., Swieszkowski, W., Annabi, N., Khademhosseini, A., Moshaverinia, A., & Tamayol, A. (2018). A Multifunctional Polymeric Periodontal Membrane with Osteogenic and Antibacterial Characteristics. *Advanced Functional Materials*, 28(3), 1–8.
<https://doi.org/10.1002/adfm.201703437>

Niknafs, B., Meskaraf-asadabadi, M., Hamdi, K., & Ghanbari, E. (2024). Incorporating bioactive glass nanoparticles in silk fibroin/bacterial nanocellulose composite scaffolds improves their biological and osteogenic properties for bone tissue engineering applications. *International Journal of*

Biological Macromolecules, 266(P1), 131167.
<https://doi.org/10.1016/j.ijbiomac.2024.131167>

Orlandi, G., Faragò, S., Menato, S., Sorlini, M., Butti, F., Mocchi, M., Donelli, I., Catenacci, L., Sorrenti, M. L., Croce, S., Segale, L., Torre, M. L., & Perteghella, S. (2020). Eco-sustainable silk sericin from by-product of textile industry can be employed for cosmetic, dermatology and drug delivery. *Journal of Chemical Technology and Biotechnology*, 95(9), 2549–2560. <https://doi.org/10.1002/jctb.6441>

Özeren, H. D., Guivier, M., Olsson, R. T., Nilsson, F., & Hedenqvist, M. S. (2020). Ranking plasticizers for polymers with atomistic simulations: PVT, mechanical properties, and the role of hydrogen bonding in thermoplastic starch. *ACS Applied Polymer Materials*. <https://doi.org/10.1021/acsapm.0c00191>

Pawar, V., & Shinde, V. (2024). Bioglass and hybrid bioactive material: A review on the fabrication, therapeutic potential and applications in wound healing. *Hybrid Advances*, 6. <https://doi.org/10.1016/j.hybadv.2024.100196>

Pihlstrom, B. L., Michalowicz, B. S., & Johnson, N. W. (2005). Periodontal diseases. *Lancet*, 366(9499), 1809–1820. [https://doi.org/10.1016/S0140-6736\(05\)67728-8](https://doi.org/10.1016/S0140-6736(05)67728-8)

Polo-Montalvo, A., Casarrubios, L., Serrano, M. C., Sanvicente, A., Feito, M. J., Arcos, D., & Portolés, M. T. (2021). Effective actions of ion release from mesoporous bioactive glass and macrophage mediators on the differentiation of osteoprogenitor and endothelial progenitor cells. *Pharmaceutics*. <https://doi.org/10.3390/pharmaceutics13081152>

Puerta, M., Arango, M. C., Jaramillo-Quiceno, N., Álvarez-López, C., & Restrepo-Osorio, A. (2019). Influence of ethanol post-treatments on the properties of silk protein materials. *SN Applied Sciences*. <https://doi.org/10.1007/s42452-019-1486-0>

- Rider, P., Kačarević, Ž. P., Elad, A., Tadic, D., Rothamel, D., Sauer, G., Bornert, F., Windisch, P., Hangyási, D. B., Molnar, B., Bortel, E., Hesse, B., & Witte, F. (2022). Biodegradable magnesium barrier membrane used for guided bone regeneration in dental surgery. *Bioactive Materials*. <https://doi.org/10.1016/j.bioactmat.2021.11.018>
- Rocha, L. K. H., Favaro, L. I. L., Rios, A. C., Silva, E. C., Silva, W. F., Stigliani, T. P., Guilger, M., Lima, R., Oliveira, J. M., Aranha, N., Tubino, M., Vila, M. M. D. C., & Balcão, V. M. (2017). Sericin from Bombyx mori cocoons. Part I: Extraction and physicochemical-biological characterization for biopharmaceutical applications. *Process Biochemistry*. <https://doi.org/10.1016/j.procbio.2017.06.019>
- Rockwood, D. N., Preda, R. C., Yücel, T., Wang, X., Lovett, M. L., & Kaplan, D. L. (2011). Materials fabrication from Bombyx mori silk fibroin. *Nature Protocols*. <https://doi.org/10.1038/nprot.2011.379>
- Sasaki, J.-I., Abe, G. L., Li, A., Thongthai, P., Tsuboi, R., Kohno, T., & Imazato, S. (2021). Barrier membranes for tissue regeneration in dentistry. *Biomaterial Investigations in Dentistry*. <https://doi.org/10.1080/26415275.2021.1925556>
- Sergi, R., Bellucci, D., & Cannillo, V. (2020). A review of bioactive glass/natural polymer composites: State of the art. In *Materials*. <https://doi.org/10.3390/ma13235560>
- Silva, A. S., Costa, E. C., Reis, S., Spencer, C., Calhelha, R. C., Miguel, S. P., Ribeiro, M. P., Barros, L., Vaz, J. A., & Coutinho, P. (2022). Silk Sericin: A Promising Sustainable Biomaterial for Biomedical and Pharmaceutical Applications. In *Polymers*. <https://doi.org/10.3390/polym14224931>
- Silva, A. V., Gomes, D. dos S., Victor, R. de S., Santana, L. N. de L., Neves, G. A., & Menezes, R. R. (2023). Influence of Strontium on the Biological Behavior of Bioactive Glasses for Bone Regeneration. In *Materials*. <https://doi.org/10.3390/ma16247654>

- Smeets, R., Knabe, C., Kolk, A., Rheinnecker, M., Gröbe, A., Heiland, M., Zehbe, R., Sachse, M., Große-Siestrup, C., Wöltje, M., & Hanken, H. (2017). Novel silk protein barrier membranes for guided bone regeneration. *Journal of Biomedical Materials Research - Part B Applied Biomaterials*. <https://doi.org/10.1002/jbm.b.33795>
- Solomon, S. M., Sufaru, I. G., Teslaru, S., Ghiciuc, C. M., & Stafie, C. S. (2022). Finding the Perfect Membrane: Current Knowledge on Barrier Membranes in Regenerative Procedures: A Descriptive Review. In *Applied Sciences (Switzerland)*. <https://doi.org/10.3390/app12031042>
- Tamjid, E., Bagheri, R., Vossoughi, M., & Simchi, A. (2011). Effect of particle size on the in vitro bioactivity, hydrophilicity and mechanical properties of bioactive glass-reinforced polycaprolactone composites. *Materials Science and Engineering C*. <https://doi.org/10.1016/j.msec.2011.06.013>
- Tan, H. W., Abdul Aziz, A. R., & Aroua, M. K. (2013). Glycerol production and its applications as a raw material: A review. In *Renewable and Sustainable Energy Reviews*. <https://doi.org/10.1016/j.rser.2013.06.035>
- Taye, M. B. (2022). Biomedical applications of ion-doped bioactive glass: a review. In *Applied Nanoscience (Switzerland)*. <https://doi.org/10.1007/s13204-022-02672-7>
- Tiyaboonchai, W., Chomchalao, P., Pongcharoen, S., Sutheerawattananonda, M., & Sobhon, P. (2011). Preparation and characterization of blended Bombyx mori silk fibroin scaffolds. *Fibers and Polymers*. <https://doi.org/10.1007/s12221-011-0324-9>
- Vallittu, P. K., Närhi, T. O., & Hupa, L. (2015). Fiber glass-bioactive glass composite for bone replacing and bone anchoring implants. In *Dental Materials*. <https://doi.org/10.1016/j.dental.2015.01.003>
- Vandrovcova, M., Hanus, J., Drabik, M., Kylian, O., Biederman, H., Lisa, V., & Bacakova, L. (2012). Effect of different surface nanoroughness of titanium

- dioxide films on the growth of human osteoblast-like MG63 cells. *Journal of Biomedical Materials Research - Part A*. <https://doi.org/10.1002/jbm.a.34047>
- Vichery, C., & Nedelec, J. M. (2016). Bioactive glass nanoparticles: From synthesis to materials design for biomedical applications. In *Materials*. <https://doi.org/10.3390/ma9040288>
- Vukajlovic, D., Parker, J., Bretcanu, O., & Novakovic, K. (2019). Chitosan based polymer/bioglass composites for tissue engineering applications. In *Materials Science and Engineering C*. <https://doi.org/10.1016/j.msec.2018.12.026>
- Wang, D., Zhou, X., Cao, H., Zhang, H., Wang, D., Guo, J., & Wang, J. (2023). Barrier membranes for periodontal guided bone regeneration: a potential therapeutic strategy. In *Frontiers in Materials*. <https://doi.org/10.3389/fmats.2023.1220420>
- Wang, K., Hazra, R. S., Ma, Q., Khan, M. R. H., Al Hoque, A., Jiang, L., Quadir, M., Zhang, Y., Wang, S., & Han, G. (2023). Robust biocompatible bacterial cellulose/silk nonwoven fabric/silk sericin sandwich membrane with strong UV-blocking and antioxidant properties. *Cellulose*. <https://doi.org/10.1007/s10570-023-05102-1>
- Wang, Y., Wang, X., Shi, J., Zhu, R., Zhang, J., & Zhang, Z. (2015). Flexible silk fibroin films modified by genipin and glycerol. *RSC Advances*. <https://doi.org/10.1039/c5ra19754f>
- Wu, J., Wang, S., Zheng, Z., & Li, J. (2022). Fabrication of Biologically Inspired Electrospun Collagen/Silk fibroin/bioactive glass composited nanofibrous scaffold to accelerate the treatment efficiency of bone repair. *Regenerative Therapy*. <https://doi.org/10.1016/j.reth.2022.05.006>
- Xu, J., Xia, Y., Song, H., Wang, L., Zhang, X., Lian, J., Zhang, Y., Li, X., Li, Y., Kang, J., Wang, X., & Zhao, B. (2023). Electrospun the oriented silk fibroin/bioactive glass @ silk fibroin/ polycaprolactone composite bi-layered membranes for guided bone regeneration. *Colloids and Surfaces A*:

<https://doi.org/10.1016/j.colsurfa.2023.132224>

Yang, Z., Wu, C., Shi, H., Luo, X., Sun, H., Wang, Q., & Zhang, D. (2022). Advances in Barrier Membranes for Guided Bone Regeneration Techniques. In *Frontiers in Bioengineering and Biotechnology*. <https://doi.org/10.3389/fbioe.2022.921576>

Yun, H., Kim, M. K., Kwak, H. W., Lee, J. Y., Kim, M. H., Kim, E. H., & Lee, K. H. (2013). Preparation and characterization of silk sericin/glycerol/graphene oxide nanocomposite film. *Fibers and Polymers*. <https://doi.org/10.1007/s12221-013-2111-2>

Yun, H., Kim, M. K., Kwak, H. W., Lee, J. Y., Kim, M. H., & Lee, K. H. (2016). The role of glycerol and water in flexible silk sericin film. *International Journal of Biological Macromolecules*. <https://doi.org/10.1016/j.ijbiomac.2015.11.016>

Zeimaran, E., Pourshahrestani, S., Djordjevic, I., Pinguan-Murphy, B., Kadri, N. A., & Towler, M. R. (2015). Bioactive glass reinforced elastomer composites for skeletal regeneration: A review. In *Materials Science and Engineering C*. <https://doi.org/10.1016/j.msec.2015.04.035>

Zhang, H., Deng, L., Yang, M., Min, S., Yang, L., & Zhu, L. (2011). Enhancing effect of glycerol on the tensile properties of bombyx mori cocoon sericin films. *International Journal of Molecular Sciences*. <https://doi.org/10.3390/ijms12053170>

Zheng, L. W., Wang, J. Y., & Yu, R. Q. (2019). Biomaterials in dentistry. In *Encyclopedia of Biomedical Engineering* (Vols. 1–3). Elsevier. <https://doi.org/10.1016/B978-0-12-801238-3.11033-5>

Zhou, W. H., & Li, Y. F. (2024). A bi-layered asymmetric membrane loaded with demineralized dentin matrix for guided bone regeneration. *Journal of the*

Mechanical Behavior of Biomedical Materials.

<https://doi.org/10.1016/j.jmbbm.2023.106230>

Zhu, H., Liu, N., Feng, X., & Chen, J. (2012). Fabrication and characterization of silk fibroin/bioactive glass composite films. *Materials Science and Engineering C*. <https://doi.org/10.1016/j.msec.2012.01.033>

Żołek-Tryznowska, Z., & Cichy, Ł. (2018). *GLYCEROL DERIVATIVES AS A MODERN PLASTICIZERS FOR STARCH FILMS*. <https://doi.org/10.24867/grid-2018-p27>